A contractile actomyosin network linked to adherens junctions by Canoe/afadin helps drive convergent extension

Jessica K. Sawyer[a,*], Wangsun Choi[a,†], Kuo-Chen Jung[a,†], Li He[b,†], Nathan J. Harris[a], and Mark Peifer[a,c]

[a]Department of Biology, University of North Carolina at Chapel Hill, Chapel Hill, NC 27599; [b]Department of Biological Chemistry, Johns Hopkins School of Medicine, Baltimore MD 21205; [c]Lineberger Comprehensive Cancer Center, University of North Carolina at Chapel Hill, Chapel Hill, NC 27599

ABSTRACT **Integrating individual cell movements to create tissue-level shape change is essential to building an animal. We explored mechanisms of adherens junction (AJ):cytoskeleton linkage and roles of the linkage regulator Canoe/afadin during *Drosophila* germband extension (GBE), a convergent-extension process elongating the body axis. We found surprising parallels between GBE and a quite different morphogenetic movement, mesoderm apical constriction. Germband cells have an apical actomyosin network undergoing cyclical contractions. These coincide with a novel cell shape change—cell extension along the anterior–posterior (AP) axis. In Canoe's absence, GBE is disrupted. The apical actomyosin network detaches from AJs at AP cell borders, reducing coordination of actomyosin contractility and cell shape change. Normal GBE requires planar polarization of AJs and the cytoskeleton. Canoe loss subtly enhances AJ planar polarity and dramatically increases planar polarity of the apical polarity proteins Bazooka/Par3 and atypical protein kinase C. Changes in Bazooka localization parallel retraction of the actomyosin network. Globally reducing AJ function does not mimic Canoe loss, but many effects are replicated by global actin disruption. Strong dose-sensitive genetic interactions between *canoe* and *bazooka* are consistent with them affecting a common process. We propose a model in which an actomyosin network linked at AP AJs by Canoe and coupled to apical polarity proteins regulates convergent extension.**

Monitoring Editor
Alpha Yap
University of Queensland

Received: May 10, 2011
Revised: May 17, 2011
Accepted: May 18, 2011

INTRODUCTION

Morphogenesis is an amazing process that converts simple tissue shapes into complex structures. It begins at gastrulation, when a ball of cells converts itself into an outline of the body, with three germ layers and defined anterior–posterior (AP) and dorsal–ventral (DV) axes. We must learn how morphogenesis is regulated at all levels: from molecular mechanisms to cellular events to tissue-level integration. During morphogenesis, cells change shape, divide, and move, all while maintaining tissue integrity. This requires coordinating cell–cell adhesion and cell shape change, events driven by cadherin-based adherens junctions (AJs) and the actomyosin cytoskeleton. Molecular mechanisms underlying this coordination remain largely mysterious. The connection was initially thought to be simple and direct, with cadherins linking to actin via β- and α-catenin, but biochemical evidence suggests otherwise (Drees *et al.*, 2005; Yamada *et al.*, 2005). Instead, recent work suggests that distinct linkers act in different events (e.g., Abe and Takeichi, 2008; Cavey *et al.*, 2008; Sawyer *et al.*, 2009); among these is the actin-binding protein Canoe (Cno; equivalent to mammalian afadin). Another important challenge is defining the roles and mechanisms of action of different linkers during distinct biological processes.

This article was published online ahead of print in MBoC in Press (http://www.molbiolcell.org/cgi/doi/10.1091/E11-05-0411) on May 25, 2011.

*Present address: Department of Biological Chemistry, Johns Hopkins School of Medicine, Baltimore MD 21205.

†These authors contributed equally to this work.

Address correspondence to: Mark Peifer (peifer@unc.edu).

Abbreviations used: AJ, adherens junction; AP, anterior–posterior; aPKC, atypical protein kinase C; Arm, Armadillo; Baz, Bazooka; Cno, Canoe; DEcad, DE-cadherin; DV, dorsal–ventral; GBE, germband extension; GFP, green fluorescent protein; MZ, maternal and zygotic; SEM, scanning electron microscopy; Sqh, Spaghetti Squash; WT, wild type.

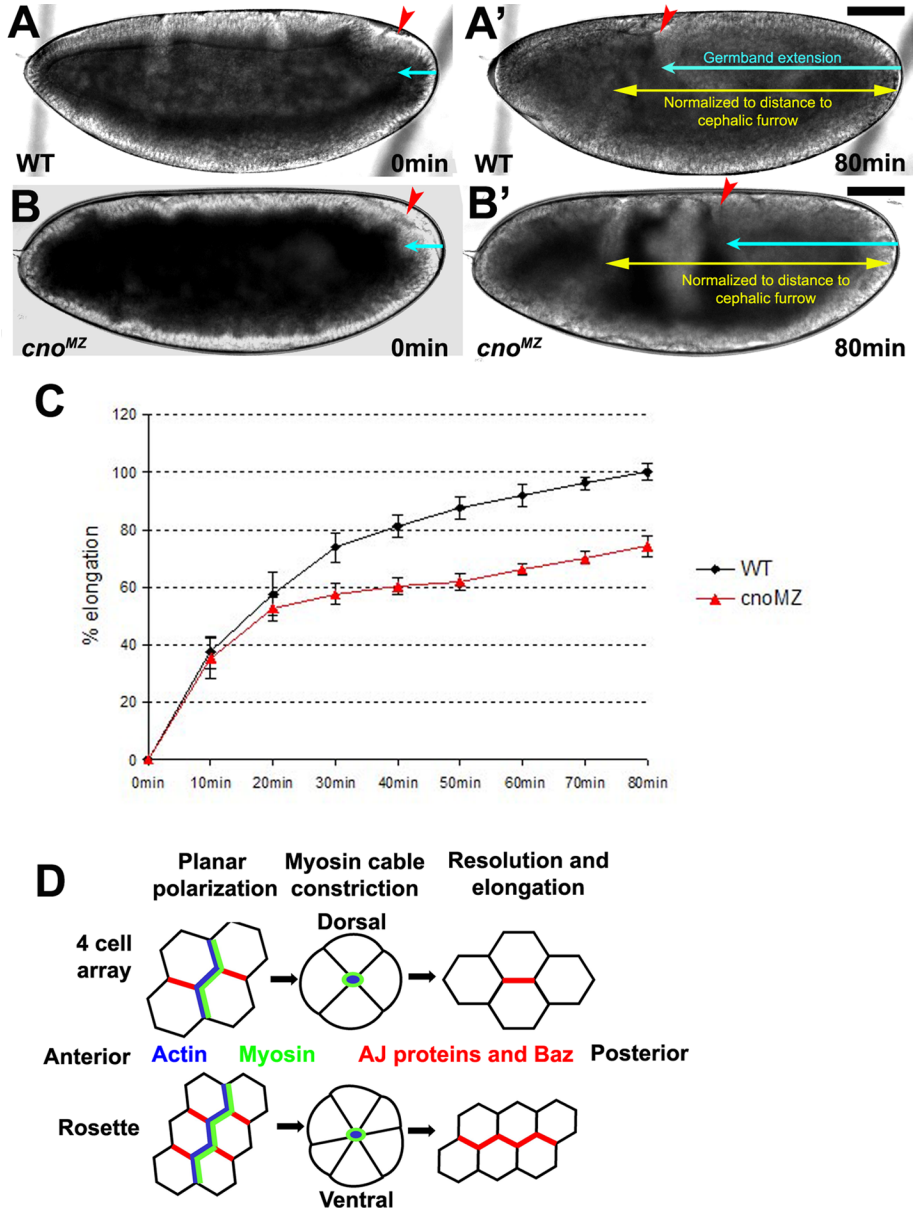

FIGURE 1: Cno loss disrupts GBE. (A, B) Embryos, anterior left. (A, A′) Stills from a movie of WT embryo. (A) t = 0. The onset of GBE, as marked by appearance of the cephalic furrow. (A′) t = 80 min; GBE is complete. Red arrowhead indicates the end of the germband. Yellow line indicates the total length from the cephalic furrow to posterior end. Blue line indicates the elongated germband. Note that at 80 min the end of the germband extends from the posterior end of the egg up around the dorsal surface to a position above and just behind the head. Bars, 20 µm. (B) *cno*^{MZ}, onset of GBE. (B′) *cno*^{MZ}, 80 min. GBE does not go to completion. Note the position of the end of the germband (red arrowhead). (C) GBE slows and does not go to completion in *cno*^{MZ} mutants. Degree of extension was normalized to embryo size using the ratio of the length of the posterior portion of the germband to the total distance from the cephalic furrow to the posterior end; WT extends 84% of this distance. In this chart, full WT GBE was thus set at 100%. WT, n = 8; *cno*^{MZ}, n = 6. Error bars = SD. (D) Diagram illustrating planar-polarization and cell intercalation in WT. Actin and myosin are enriched at AP borders, and AJ proteins and Baz are enriched at DV borders. Contraction of myosin cables is thought to drive cell intercalation.

Apical cell constriction during *Drosophila* mesoderm internalization provides a model of cell shape change during morphogenesis. Although the textbook model of apical constriction involves constriction of a circumferential belt of actin filaments underlying cell–cell AJs, recent work has revealed that this is not always the case. Instead, in the fly mesoderm and amnioserosa, cell fate cues initiate a signaling pathway triggering assembly and constriction of an apical actomyosin network covering the surface of each cell (Harris *et al.*, 2009). This network constricts in a cyclical manner, with an unidentified molecular ratchet driving progressive cell shape change (Martin *et al.*, 2009; Solon *et al.* 2009). Cell shape change requires that the contractile network be connected to AJs (Dawes-Hoang *et al.*, 2005). AJs also join cells, transmitting forces from cell to cell across epithelial sheets. Tissue-level integration plays a key role in mesoderm invagination. Forces transduced via AJs across the tissue modify individual cell shape changes, as cells respond both to internally generated contractile forces and those generated by the supracellular network (Martin *et al.*, 2010).

Although it was clear that linkage of the apical contractile network to AJs is crucial for mesoderm apical constriction, the molecular linkage initially remained unclear. We previously explored the role of Cno in this process. Cno interacts with nectins and other AJ proteins and was suggested to play important roles in mammalian cell adhesion (Takai *et al.*, 2008). We found Cno is not essential for *Drosophila* cell adhesion but is required for proper mesoderm invagination (Sawyer *et al.*, 2009). In Cno's absence, the apical actomyosin network constricts and cells initiate shape change, but then the network detaches from AJs, preventing effective mesoderm invagination. These data suggested that Cno mediates or regulates attachment between the actomyosin cytoskeleton and cell–cell AJs during mesoderm apical constriction.

Here we explore coordination of the actomyosin cytoskeleton and AJs during a very different cell behavior: convergent extension, in which cells intercalate between one another in the plane of the epithelium to elongate the body axis (Harris *et al.*, 2009; Yin *et al.*, 2009). This morphogenetic movement is also common to gastrulation in many animals but is thought to be cell biologically and mechanistically very different from apical constriction, although myosin regulation is also critical.

In *Drosophila* this process is called germband extension (GBE) (Figure 1, A and A′; Zallen and Blankenship, 2008). During GBE the embryo elongates twofold along the AP axis while narrowing along the DV axis. Because embryos are constrained within the eggshell, this leads to the posterior end of the embryo moving from the posterior end of the egg (Figure 1A, red arrowhead) up around the dorsal side to lie above the head (Figure 1A′, red arrowhead). Elongation in the first few minutes is driven at least in part by oriented cell division (da Silva and Vincent, 2007) and relaxation of DV cell elongation caused

by mesoderm invagination (Butler *et al.*, 2009). In our current view, extension during the rest of GBE is dominated by intercalation of ectodermal cells (Figure 1D; Irvine and Wieschaus, 1994). As GBE initiates, cells become planar polarized, with AJ proteins and Bazooka (= Par3) enriched along DV borders and actin and nonmuscle myosin II (myosin) enriched along AP borders (Figure 1D, left; note that they are not lost from the other borders). Myosin enrichment leads to formation of myosin cables extending across several cell diameters. Their constriction shrinks AP borders, driving intercalation and elongating the ectoderm (Figure 1D; Zallen and Wieschaus, 2004; Blankenship *et al.*, 2006; Rauzi *et al.*, 2008; Fernandez-Gonzalez *et al.*, 2009). Consistent with this, zygotic myosin is required for full GBE (Bertet *et al.*, 2004). Thus cell shape changes and myosin arrangement during GBE are thought to be quite distinct from those during apical constriction.

Given the important role of Cno in apical constriction during mesoderm invagination, we explored whether it plays roles in subsequent morphogenetic events. We found that Cno is required for completion of GBE. In analyzing Cno's role, we discovered surprising parallels between GBE and mesoderm apical constriction in wild-type embryos. Ectodermal cells are covered by an oscillating apical network of actin and myosin that drives periodic cell constriction. Furthermore, this coincides with progressive elongation of ectodermal cells along the AP axis, contributing to body axis elongation. In Cno's absence, the apical actomyosin network detaches from cell–cell junctions in a planar-polarized way. This disrupts coordination of apical myosin constriction and cell shape change, blunting elongation of cells along the AP axis. Loss of Cno also leads to dramatic changes in localization of the apical polarity proteins Bazooka (Baz) and atypical protein kinase C (aPKC), which correlate with changes in myosin localization. We propose a model in which a contractile apical actomyosin network plays an important role in driving body axis elongation during convergent extension, with Cno helping to maintain network:AJ connections in a planar-polarized manner and thus coordinate contractility and cell shape change.

RESULTS

Cno loss disrupts GBE

For actomyosin contractility to be coupled to cell shape change, it is important that the cytoskeleton is anchored at cell–cell AJs. Given Cno's importance in linking AJs and the actomyosin cytoskeleton during mesoderm apical constriction (Sawyer *et al.*, 2009), we explored whether Cno loss affects GBE, comparing GBE speed and extent in wild-type (WT) flies and maternal/zygotic null cno^{R2} mutants (cno^{MZ}). We imaged live for 80 min from cephalic furrow initiation to the end of WT GBE. During the first 10 min of GBE, WT flies and cno^{MZ} mutants extend at similar rates, but then cno^{MZ} mutants slow significantly and fail to complete GBE (Figure 1C). cno^{MZ} mutants only extend 74% as far as WT flies (Figure 1, A–C). The midgut is still internalized in cno^{MZ} mutants (Sawyer *et al.*, 2009), suggesting that midgut invagination failure is not what blocks elongation. These data demonstrate that Cno plays an important role in GBE, with its loss disrupting GBE to a degree similar in extent to that seen in *baz* or *zipper* (myosin heavy chain) zygotic mutants (Bertet *et al.*, 2004; Zallen and Wieschaus, 2004).

An apical contractile actomyosin network during germband extension

During GBE, the ectoderm lengthens approximately twofold in the AP axis and narrows in the DV axis. In the current view, this is largely driven by cell intercalation (Figure 1D; Irvine and Wieschaus, 1994), with important contributions from DV cell relaxation (Butler *et al.*, 2009) and oriented cell division (da Silva and Vincent, 2007) during the first 10 min (Figure 1C). Cytoskeletal and AJ proteins become reciprocally planar polarized during GBE (Bertet *et al.*, 2004; Zallen and Wieschaus, 2004) (Figure 1D), with actin and myosin enriched on AP borders and AJ proteins enriched on DV borders. Myosin planar polarization triggers formation of myosin cables, often extending several cell diameters (Figure 2A, arrowheads), constriction of which helps drive intercalation (Figure 1D) (Blankenship *et al.*, 2006; Rauzi *et al.*, 2008; Fernandez-Gonzalez *et al.*, 2009).

We reexamined the dynamic localizations of myosin and AJs during WT GBE. The planar-polarized myosin cables that others previously reported were easily observed (Figure 2A), but we were surprised to find that myosin was not confined to AJs. Instead the apical surface of each ectodermal cell was covered by a dynamic myosin network (Figure 2B and Supplemental Movie S1) resembling that in apically constricting mesoderm (Martin *et al.*, 2009). Our live imaging revealed that, as in mesoderm, myosin spots and filaments formed on the apical surface, coalesced by constriction, and dissipated (Figure 2C, arrowheads). Thus. despite major differences in cell shape changes during mesoderm invagination and GBE, both share an apical contractile network. While this article was in preparation, Rauzi *et al.* (2010) and Fernandez-Gonzalez and Zallen (2011) independently identified and characterized this contractile apical actomyosin network.

In fact, individual germband cells go through multiple rounds of myosin network formation, constriction, and dissipation (Figure 2D, cell undergoing six rounds; Supplemental Movie S1, asterisk). Double imaging with DE-cadherin–GFP (DEcad-GFP) revealed that pulses of myosin constriction coincided with periodic decreases in apical cell area (Figure 2D), suggesting that the network is coupled to AJs. We used automated analysis of many cells (He *et al.*, 2010) to quantitate this. This also revealed periodic pulses of apical myosin accumulation and of cell shape change in individual cells (Figure 3A); the amount of apical myosin accumulation and the degree of change in cell area varied between pulses, as was previously observed in the *Drosophila* mesoderm and amnioserosa (Martin *et al.*, 2009; Solon *et al.*, 2009). When we calculated the rate of change in these two parameters, we found the peaks of apical myosin change and cell area change to be more regular (Figure 3C). Apical myosin pulses peaked every 162 ± 44 s (Figure 3E). This regularity was also revealed by autocorrelation analysis of individual apical myosin peaks; in addition to the correlation of a peak with itself, there were also clear peaks offset by ~160 s (Figure 3, G and I, arrows). Finally, this analysis revealed a strong correlation between the timing of pulsatile increases of apical myosin and timing of cell constriction (Figure 3, J, arrow, L, and M). Myosin increase slightly preceded constriction (by ~6.5 s; Figure 3, J and L), consistent with the hypothesis that myosin contractility drives cell constriction. This hypothesis is reinforced by instances in which myosin cables bridging AJs at different cortical points appeared to exert force and alter cell shape (Figure 2E, arrowheads; Supplemental Movie S2). Together, these data reveal a surprising parallel between cells undergoing convergent extension during GBE and cells undergoing apical constriction: both share a contractile apical actomyosin network undergoing pulsatile constriction.

A novel cell shape change—AP cell elongation—coincides with cycles of actomyosin contraction

The cyclical pulses of myosin contractility in the mesoderm lead to progressive apical constriction (Martin *et al.*, 2009). We thus tested the hypothesis that cyclical constriction of ectodermal cells also coincides with progressive cell shape change. At gastrulation onset,

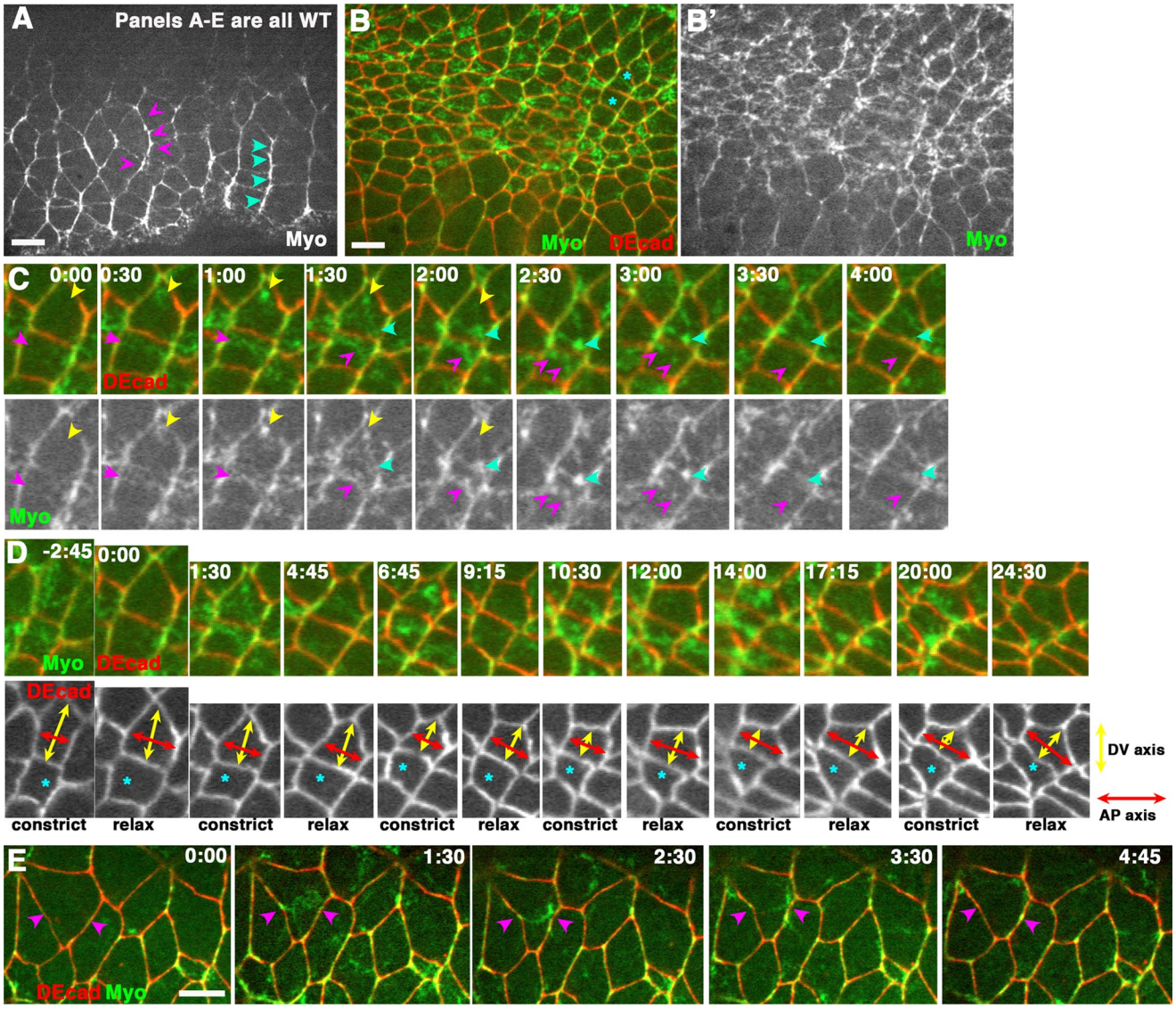

FIGURE 2: An apical contractile actomyosin network and cell shape change during GBE. WT embryos expressing DEcad-GFP (red) and myosin light chain–mCherry (green; = Spaghetti Squash [sqh]), stage 7. In all figures, unless noted, embryos are anterior left, dorsal up, with antigens and genotypes indicated. (A) Arrowheads indicate myosin cables at AJs. (B) Apical view, contractile actomyosin network (asterisks indicate cells in C and D). (C–E) Movie stills, with time in minutes:seconds. (C, D) Single pair of cells. (C) Arrowheads indicate myosin condensations forming and dissipating. (D) Multiple cycles of contraction and relaxation coincide with progressive elongation of cells along the AP body axis (red arrows). (E) Myosin cable forms and constricts cell (arrowheads). Bars, 5 μm.

cells begin as isometric and hexagonal (Zallen and Zallen, 2004), but mesoderm invagination drives substantial elongation of ectoderm cells along the DV axis, especially near the ventral midline. During the first 10 min of GBE, these cells then return to a more isometric shape (Butler *et al.*, 2009).

We observed a second novel, spatially distinct cell shape change during the period of pulsatile contractions in germband cells. Although cell areas increased after each round of myosin dissipation (Figure 2D), over multiple rounds cells underwent a progressive change in cell shape. This lengthened cells along the AP axis (Figure 2D, arrows; Supplemental Movie S1, asterisk; later we refer to this as AP cell elongation).

This change in individual cell length could contribute to the elongation of the entire tissue. To test this hypothesis and to determine the average amount of cell elongation during this process, we quantitated changes in cell shape and apical area in many cells between the end of cellularization and the middle of GBE. We compared lengths of AP and DV cell borders and assessed apical cell area (Supplemental Figure S1, A and B). To remove bias, we measured all borders and used ImageJ to classify borders as AP or DV (Supplemental Figure S1, legend). Before mesoderm invagination, cells are isometric, with equal AP and DV border lengths (mean AP:DV border = 2.6:2.6 μm; Supplemental Figure S2, A and E, left). As GBE and pulsatile ectodermal cell constriction begins, cells elongated approximately twofold along the AP axis (elongating DV cell borders). In contrast, cell length along the DV axis (and thus AP cell borders) remains constant (mean AP:DV border = 2.5:4.3 μm; Supplemental Figure S2, B and E, right). As a result of cell elongation, the apical area of cells increases ~50% (Supplemental Figure S2,C and D). These changes parallel those we observed in individual cells (Figure 2D, arrows). These data are consistent with the hypothesis that this novel cell shape change—AP cell elongation—helps

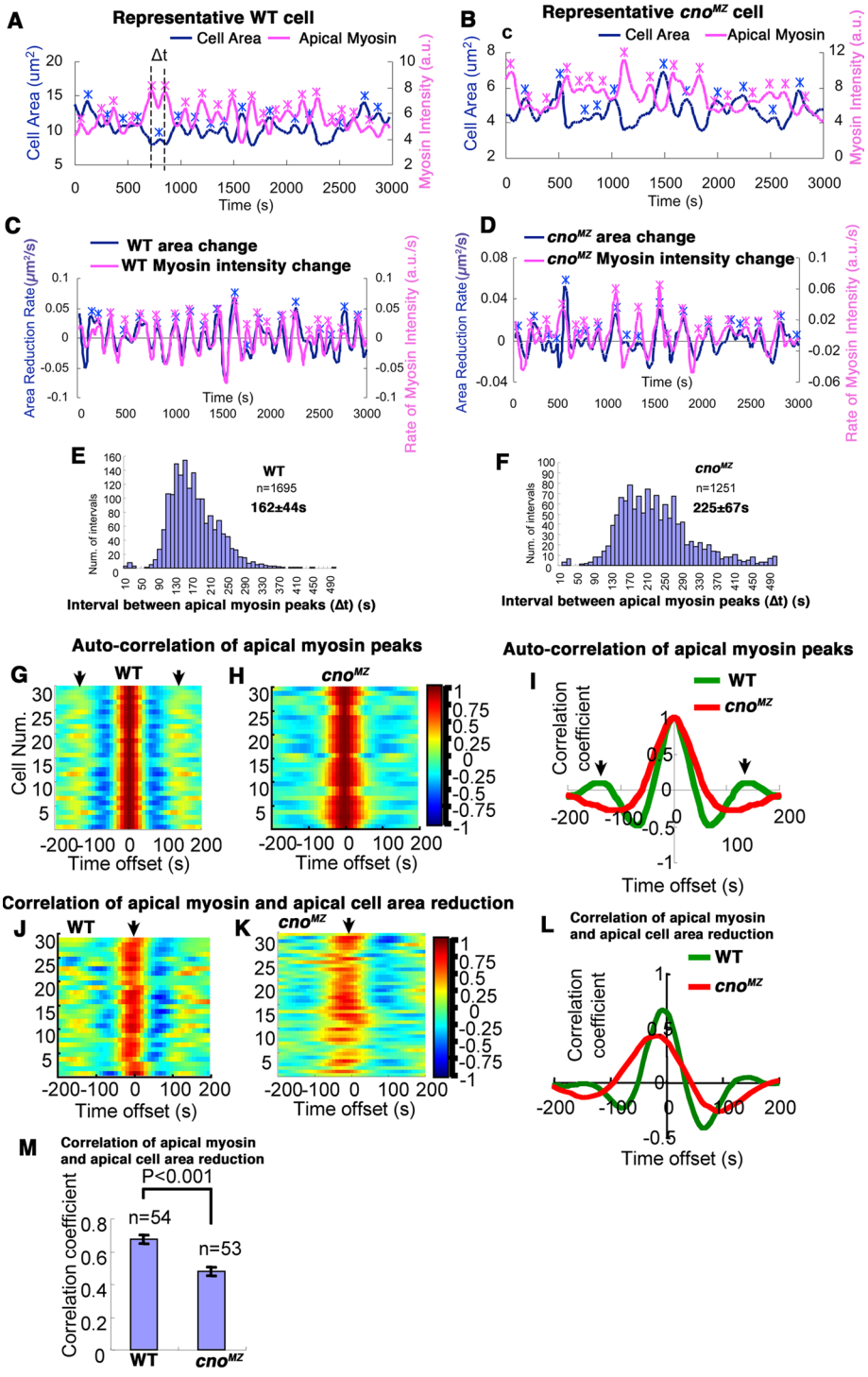

FIGURE 3: Automated analysis reveals correlated apical myosin accumulation and cell constriction in WT and a reduced correlation in *cno*^{MZ} mutants. (A, B) Cells undergo periodic changes in apical myosin accumulation and cell area. Cell surface area (blue line) and apical myosin intensity (Sqh-mCherry intensity; pink line) of one representative WT (A) or *cno*^{MZ} (B) cell over time. Asterisks indicate positions of peaks recognized by MATLAB. Δt is the time interval between neighboring peaks. (C, D) Rate of change of apical cell area (blue line) and apical myosin intensity (pink line). These are the same cells analyzed in A and B. (E, F) Histograms showing time intervals between neighboring apical myosin peaks in WT (E) and *cno*^{MZ} (F). In *cno*^{MZ} the time between peaks lengthens and the regularity of peaks diminishes. (G, H) Autocorrelation coefficient of the rate of apical myosin intensity changes in WT (G) and *cno*^{MZ} mutant (H). Each row shows the correlation from a different cell as a function of time offsets from −200 to 200 s. The correlation coefficient (r) from −1 to 1 was color coded according to the scale on the left color bar. (I) Averaged autocorrelation coefficients of apical myosin intensity from 54 WT cells (green line) and 53 *cno*^{MZ} mutant cells (red line) plotted with different time offsets. The curve of WT cells shows clear peaks around ±150 s (arrows), which were lost in *cno*^{MZ}. This result suggests periodic activity in WT is more regular than in *cno*^{MZ} mutants, which is consistent with the broader distribution of Δt in *cno*^{MZ}. (J, K) The r's between cell surface area reduction and the rate of apical myosin intensity change in WT (J) and *cno*^{MZ} (K). Each row shows the correlation from a different cell as a function of various time offsets. (L) Averaged r's between cell area reduction and apical myosin intensity change from 54 WT cells (green line) and 53 *cno*^{MZ} cells (red line). Both showed a negative shift (−6.5 s for WT and −17.5 s for *cno*^{MZ}), suggesting that in both situations myosin changes preceded the cell area activity. The increased time shift between myosin and cell area in *cno*^{MZ} might be a consequence of weakened mechanical linkage. (M) The average maximum r's between area reduction and apical myosin intensity change of WT and *cno*^{MZ} plotted in a bar graph for comparison. p value was calculated by Student's *t* test. Reduction of the maximum r suggested that Cno loss weakened the linkage between cell area dynamics and myosin activity.

elongate *the tissue* along the AP axis during GBE (Supplemental Figure S3C). Perhaps the same planar-polarized myosin cables that help drive cell intercalation (Supplemental Figure S3, A and B, double-headed arrows) also constrain cell elongation along the DV axis and thus restrict it to the AP axis.

During GBE, myosin detaches from AJs in a planar-polarized way in *cno*^{MZ} mutants

Because Cno is required for effective GBE (Figure 1C), we next explored the cell biological effects of Cno loss. On the basis of its known roles, we tested two hypotheses. Cno might regulate linkage between the actomyosin cytoskeleton and AJs during GBE, or it could regulate cell–cell adhesion. Consistent with the first hypothesis, myosin localization was dramatically altered in the lateral ectoderm of *cno*^{MZ} mutants during GBE. As in WT, myosin became planar-polarized early in GBE, enriched along AP borders. In WT, a single myosin cable colocalized with AP AJs (Figure 4, A and J, arrows), suggesting that cables in adjacent cells are very closely opposed. In contrast, in *cno*^{MZ} mutants, we saw two distinct myosin cables at AP cell borders that remained at the apical cortex but separated from one another (Figure 4B, between arrows; single myosin cables were seen at DV borders). This suggests that the myosin networks in adjacent cells detached from AJs, retracting unto the apical surface. These separated myosin

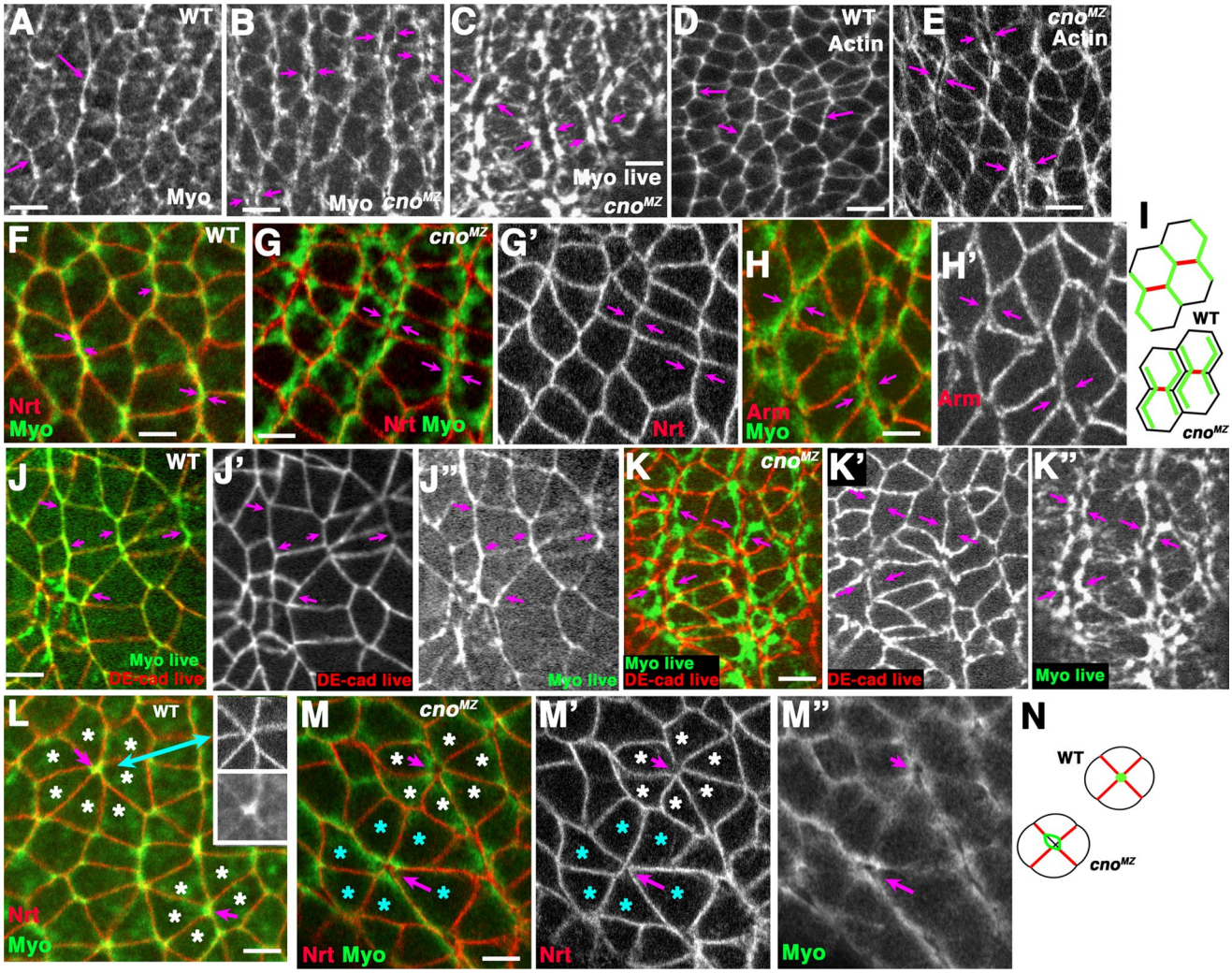

FIGURE 4: Cno loss leads to planar-polarized detachment of the apical actomyosin network. Embryos, stage 7. Fixed (A, B) or live (C) embryos. Contrast the single myosin cable on AP borders in WT (A, arrows) with the detached cables on AP borders in *cno*^{MZ} (B, C, arrows). (D, E) Cortical actin (D, arrows) is also detached at some AP borders in *cno*^{MZ} (E, arrows). (F–K) WT myosin cables colocalize with Nrt (F, arrows) and DEcad (J) at cell borders. In *cno*^{MZ}, Nrt (G, arrows), Arm (H, arrows), and DEcad (K, arrows) localize between detached myosin cables. (L–N) In WT, myosin localizes to rosette vertices (L, arrows indicate vertices, asterisks indicate cells in rosettes), whereas in *cno*^{MZ} myosin localizes in rings around vertices (M, arrows). I and N illustrate these changes diagrammatically. Bars, 5 μm.

cables were also apparent in live imaging with myosin-mCherry (Figure 4C, between arrows; Supplemental Movie S3). F-actin exhibited similarly altered localization; WT cortical cables (Figure 4D, arrows) sometimes appeared detached in *cno*^{MZ}, forming parallel cables (Figure 4E, between arrows). Detached myosin cables were seen throughout the germband during early GBE (Supplemental Figure S4, A and B; unless noted, phenotypes were highly penetrant—quantitation is in Supplemental Table S3). Myosin separation from AJs was also quite striking in rosettes, where multiple cell vertices meet. Normally, myosin localizes tightly to vertices (Figure 4L, magenta arrow, insets). In contrast, in *cno*^{MZ}, myosin instead formed rings around vertices (Figure 4M, arrows). Despite these dramatic changes, an apical myosin network remained, in which myosin condensations formed and dissipated (Supplemental Figure S4E, arrows; Supplemental Movie S3). Together these data suggest that Cno plays a specific, planar-polarized role in attaching the apical myosin network and junctional myosin cables to AP cell borders and to cell vertices during GBE.

Myosin cable detachment is not due to cell separation

The simplest hypothesis to explain these observations is that Cno regulates linkage between the actomyosin cytoskeleton and AJs during GBE, as it does during mesoderm apical constriction (Sawyer *et al.*, 2009). However, we first needed to rule out an alternate hypothesis: that in Cno's absence, cell adhesion is compromised, causing cells to separate. AJs assemble normally in *cno*^{MZ} mutants, and in dorsal ectodermal cells AJs are maintained through the end of morphogenesis, making this possibility less likely (Sawyer *et al.*, 2009). To rule out more subtle changes in cell adhesion, we explored whether cells separate, using scanning electron microscopy (SEM). Cells went from rounded during cellularization (Supplemental Figure S5, A and B) to more tightly adherent during early GBE (Supplemental Figure S5, C and E vs. D, F, and G), with no discernible differences between *cno*^{MZ} and WT. As GBE progresses, mitotic domains in the lateral and ventral ectoderm begin mitosis, and those cells round up in WT and mutants. However, cells that had not yet divided remained similarly adherent in WT and *cno*^{MZ}

(Supplemental Figure S5, H vs. I). Thus substantial cell separation does not explain myosin detachment in *cno*^{MZ} mutants.

We also analyzed lateral and AJ markers. In WT, the basolateral protein Nrt directly underlies the single myosin cable (Figure 4F, arrows). In *cno*^{MZ} a single Nrt-stained cell border (Figure 4G, between arrows) remained between the two myosin cables, supporting the idea that cells did not substantially separate. We also examined the relationship between AJs and myosin cables. WT myosin cables colocalize with AJ proteins like DEcad (Figures 2E and 4J, arrows). In contrast, in *cno*^{MZ} mutants, myosin cables separated from AJs (Figure 4, H and K; as observed both in fixed embryos using Armadillo [fly βcat] as an AJ marker and via live imaging, using DEcad-GFP). Armadillo (Arm) and DEcad remained as a single border at AJs between detached myosin cables (Figure 4, H and K, between arrows; Supplemental Movie S3). Together, our data support the hypothesis that myosin cables detach primarily due to weakened AJ:actomyosin network linkages, not cell separation

We examined AJs and myosin further, exploring their relationship along the apical–basal axis. WT cortical myosin cables and AJs are in the same plane (Figures 2E and 4J, arrows). In contrast, detached myosin cables in *cno*^{MZ} are more apical than the AJs from which they detached. In the apical plane where detached myosin cables reside, gaps and discontinuities in Arm localization are sometimes observed (Supplemental Figure S4B, purple arrows). However, at the level of the AJs (1.5 µm more basal), Arm was substantially more continuous (Supplemental Figure S4C, purple arrows). Other apparent apical discontinuities in Arm localization occur at cell vertices where multiple cells meet (Supplemental Figure S4, B and C, yellow asterisks and arrows; abnormal cell arrangements at vertices were also seen in SEM; Supplemental Figure S4D, arrows). Together, these data suggest that Cno helps link the actomyosin network tightly to AP AJs and at multicellular junctions, and that in its absence the network detaches.

Cno loss reduces coupling between the apical actomyosin network and cell shape change

These dramatic changes in linkage of the apical actomyosin network in *cno*^{MZ} mutants provide a possible mechanistic explanation of the defects seen in GBE—perhaps tight linkage is critical for coupling apical actomyosin contractility and cell shape change. To test this hypothesis, we analyzed the effects of Cno loss on periodic contractions of the actomyosin network and on cell shape change, by automated analysis of many cells. *cno*^{MZ} cells retained a contractile apical myosin network that underwent cycles of appearance and dissipation (Figure 3, B and D), suggesting that tight AP connections of the network to AJs are not essential for maintaining this process. However, pulses of apical myosin became significantly less frequent and less regular in periodicity than in WT (225 ± 67 s vs. 162 ± 44 s in WT; Figure 3, C vs. D, E vs. F, G vs. H, I). Furthermore, the correlation between pulses of apical myosin and periodic changes in cell shape was significantly reduced (Figure 3, J vs. K, L, M). These data suggest that attachment of the actomyosin network to AP cell boundaries mediated by Cno is important for the fidelity and coupling of periodic pulses of apical actomyosin and periodic cell shape change.

The WT data suggest that the pulsatile changes in cell shape coincide with a novel progressive cell shape change that contributes to GBE: cell elongation along the AP body axis (Supplemental Figure S2E). We hypothesized that disruption of the fidelity and coupling of actomyosin contractility and shape change seen in *cno*^{MZ} mutants might disrupt AP cell elongation. We found that in *cno*^{MZ} mutants cell elongation along the AP axis is significantly reduced (Supplemental Figure S2B; cell elongation along the AP axis elongates DV cell borders), leading to reduced cell shape anisometry during early GBE (DV-to-AP cell border ratio is 1.41 vs. 1.70 in WT). This fits in well with the reduction of GBE we observed in *cno*^{MZ}. Failure to fully extend cells along the AP axis also resulted in smaller apical areas of *cno*^{MZ} cells (Supplemental Figure S2D). Thus Cno loss reduces normal asymmetric cell elongation, supporting a mechanism in which anchoring of the actomyosin network along AP borders may help drive GBE.

We also examined the effects of Cno on the other shape change, which occurs during the first 10 min of GBE, in which ectodermal cells that were stretched along the DV body axis by mesoderm invagination relax to an isometric shape (Butler *et al.*, 2009). In contrast to AP cell elongation, this cell shape change does *not* require Cno. *cno*^{MZ} mutants elongate as rapidly as WT during the first 10 min of GBE (Figure 1C), when DV relaxation plays an important role (Butler *et al.*, 2009). Furthermore, live imaging confirmed that DV relaxation still occurs in *cno*^{MZ} mutants (Supplemental Figure S6, A vs. B).

Although Cno plays a clear role in AP cell elongation, the effects of Cno loss on tissue-level rearrangements are more complex. Mutant cells retain some ability to change shape, and detached myosin cables still appear able to drive cell rearrangements, shrinking AP boundaries (Supplemental Figure S3, D–F, blue, red, and yellow arrows, G vs. H), but there are clear delays in GBE (Figure 1). In the future it will be important to explore in detail how Cno loss affects the entire suite of cell behaviors driving GBE.

The apical myosin network in the ectoderm detaches from AJs in *cno*^{MZ} mutants, but spot connections remain

One puzzling feature of the detachment of myosin from AP AJs in *cno*^{MZ} mutants is that the detached myosin cables remain within a few microns of AJs. This contrasts with what we observed in the mesoderm, where the detached apical actomyosin network constricted to a ball (Sawyer *et al.*, 2009; Supplemental Figure S4, F and G, arrows). We hypothesized that this might reflect residual, Cno-independent connections between AJs and the apical actomyosin network in the ectoderm. To test this, we compared progression of detachment in the invaginating mesoderm and the germband. Live imaging of invaginating mesoderm revealed DEcad-containing membrane strands (Supplemental Figure S4G, arrowheads) extending between myosin balls (Supplemental Figure S4G, arrows), suggesting residual network:AJ connections exist in this tissue. These were also visible in SEM (Supplemental Figure 4H; similar membrane strands were seen in cells with reduced AJ function; Martin *et al.*, 2010). Thus, in mesoderm, residual AJ:network connections exist but are not sufficient to resist constriction of the apical myosin network.

We then explored lateral ectoderm cells that participate in GBE. In *cno*^{MZ} mutants, during early GBE, the apical myosin network in ectodermal cells separated from AJs but did not collapse into balls as it did in the mesoderm. Instead, myosin initially formed rings just inside AJs (e.g., Figure 5A, arrows; Supplemental Movie S4), consistent with remaining connections between the network and AJs. These myosin rings went through cycles of formation, constriction, and dissipation (e.g., Figure 5B, cell 1, arrows; Supplemental Movie S4). Cells also periodically changed shape (Figure 5B′; cells 1–3 constrict and then relax, whereas cell 4 starts constricted and relaxes; Supplemental Movie S4), consistent with the possibility that some connection remains between network and AJs. A third observation also supported a remaining connection. Along the basolateral cell surface, cortical DEcad was smooth (Figure 5, C and D basal), as in

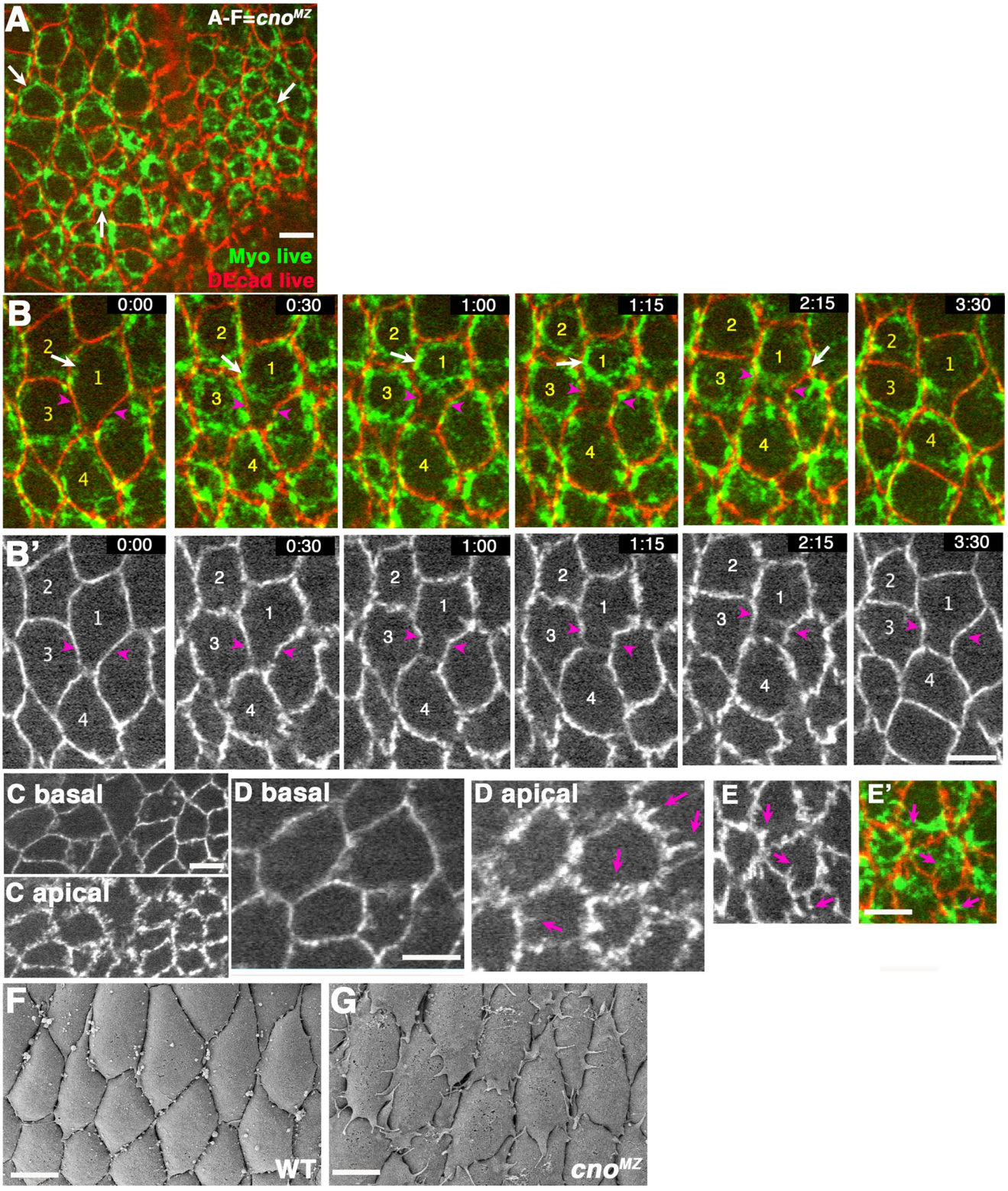

FIGURE 5: After Cno loss, apical actomyosin retains connections with AJs in the ectoderm. (A–E) *cno*^{MZ}, DEcad-GFP and myosin(Sqh)-mCherry. Lateral ectoderm soon after mesoderm invagination. (A) Myosin rings detach from AJs but do not constrict to balls (arrows), in contrast to the mesoderm. (B) Movie stills from Supplemental Movie S4; time is in minutes:seconds. Myosin rings appear and disappear (B, arrows). Cells 1–3 constrict and then relax (e.g., B′, arrowheads), whereas cell 4 relaxes. (C, D) Apical and more-basolateral sections of lateral ectoderm in *cno*^{MZ}mutants. Apically DEcad-containing membrane is stretched into strands (D, arrows), whereas 1 µm basally it is more continuous. (E) Strands are often embedded in myosin rings (arrows). (F, G) SEM also reveals membrane strands in *cno*^{MZ} (G), which are not observed in WT (F). Bars, 5 µm.

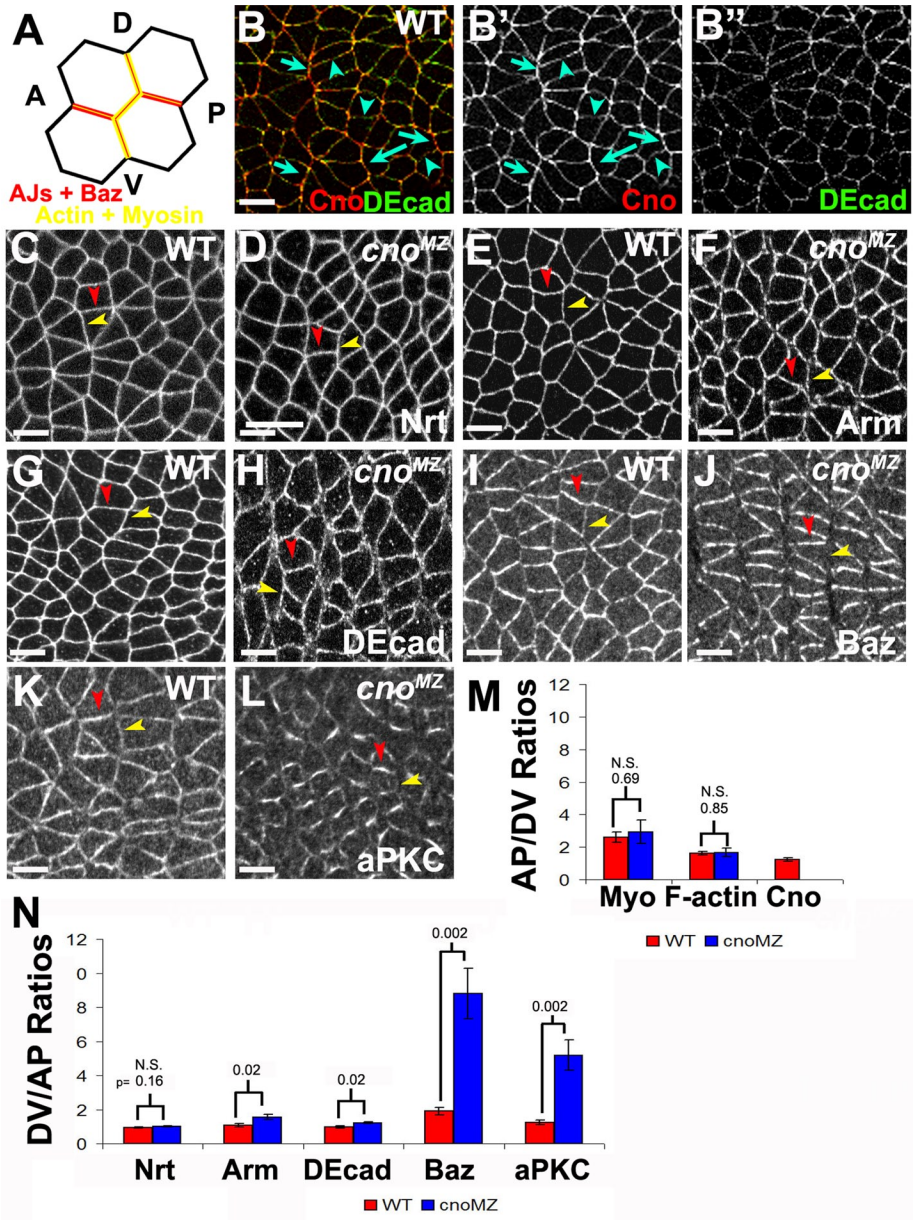

FIGURE 6: Cno loss does not affect cytoskeletal planar polarity but enhances planar polarity of AJ and apical polarity proteins. (A) Diagram; actin/myosin are enriched on AP borders (yellow), and junctional proteins are enriched on DV borders (red). (B–L) Stage 7. (B) Cno is enriched on AP (arrows) relative to DV borders (arrowheads). (C–L) Planar polarity, WT vs. *cno*^{MZ}. Red arrowheads indicate DV borders. Yellow arrowheads indicate AP borders. (C, D) Nrt is not planar polarized in either genotype. (E–H) Cno loss subtly enhances Arm and DEcad planar polarity. (I–L) Cno loss dramatically accentuates Baz and aPKC planar polarity. Bars, 5 µm. (M, N) Quantitation of planar polarity in *cno*^{MZ} mutants vs. WT.

WT. However, in the apical-most plane where DEcad was visible (1 µm more apical), the cortex appeared very convoluted, with membrane strands less dramatic but reminiscent of those in mesoderm (Figure 5, C and D apical, arrows). Strands were often embedded in the apical myosin network, as if they remained attached to it (Figure 5E, arrows). These strands were also visible in SEM (Figure 5, F vs. G). Together, these data suggest that Cno helps maintain tight connections between the apical actomyosin network and AJs in the ectoderm but that other proteins mediate residual spot connections. Furthermore, the effects of Cno loss during GBE suggest that Cno has a planar-polarized role in maintaining AJ:network linkages during GBE, whereas in the mesoderm its role is uniform around the cell.

Cno is planar polarized with cytoskeletal rather than AJ proteins

Given the striking planar-polarized defects in the actomyosin network during GBE in *cno*^{MZ}, we examined whether Cno is planar polarized in this process. Cno largely colocalizes with AJs from gastrulation onset (Sawyer *et al.*, 2009), suggesting the hypothesis that during GBE it would become enriched on DV cell borders like the AJ proteins. However, unlike DEcad, Cno is enriched at tricellular junctions with a subset of actin (Sawyer *et al.*, 2009), and its effects on myosin attachment are most dramatic at AP cell borders, where myosin and actin are enriched, consistent with the alternate hypothesis that it would colocalize with cytoskeletal proteins. To determine whether Cno is planar polarized, we immunostained WT embryos, measured the mean fluorescence intensity of Cno on all cell borders, and then compared borders aligned along AP or DV axes of the embryo (AP borders 0°–29° vs. DV borders 60°–90°; Supplemental Figure S1). Of interest, Cno is enhanced on AP borders with myosin and F-actin, rather than being enriched along DV borders with other AJ proteins (AP/DV = 1.20; Figure 6B, arrows vs. arrowheads; also see Figure 6M and Table 1). This is consistent with the planar-polarized myosin detachment we observed in *cno*^{MZ}, supporting the hypothesis that Cno plays a particularly important role in regulating linkage between AJs and apical actomyosin along AP borders.

Cytoskeletal planar polarity is not altered in *cno*^{MZ}

During GBE, myosin and actin become enriched on AP borders (Bertet *et al.*, 2004; Zallen and Wieschaus, 2004; Blankenship *et al.*, 2006). This is thought to help drive GBE. Given the dramatic, polarized disruption of the apical actomyosin network in *cno*^{MZ}, we initially hypothesized that Cno loss would alter cytoskeletal planar polarity, reducing asymmetric accumulation along AP cell borders. In our previous studies we noted in passing that Arm and myosin planar polarity might be altered in *cno*^{MZ} (Sawyer *et al.*, 2009). To examine this in detail, we quantitated junctional and cytoskeletal planar polarity in WT and *cno*^{MZ} during early GBE, comparing protein ratios on AP/DV borders to remove variation between experiments due to differential staining. It was surprising that Cno loss had no effect on planar polarization of myosin or F-actin. They were similarly enriched on AP borders in *cno*^{MZ} and WT (Figure 6M; in contrast, Nrt is not planar polarized in WT or *cno*^{MZ}; Figure 6, C, D, and M, Table 1, and Supplemental Table S1). Thus detachment of the actomyosin network from AP AJs does not affect myosin's

Protein	Ratio[a]	Ratio[a]	p value for differences in degree of planar polarity[b]	
WT vs. *cno^{MZ}*				
	WT DV/AP	*cno^{MZ}* DV/AP	WT vs. *cno^{MZ}*	
Nrt	0.94 ± 0.03	0.96 ± 0.03	0.157	
Arm	1.08 ± 0.09	1.56 ± 0.14	0.021	
DEcad	0.98 ± 0.06	1.23 ± 0.05	0.015	
aPKC	1.26 ± 0.14	5.19 ± 0.89	0.002	
Baz	1.91 ± 0.22	8.81 ± 1.48	0.002	
	WT AP/DV	*cno^{MZ}* AP/DV		
Myosin	2.61 ± 0.33	2.93 ± 0.71	0.688	
F-Actin	1.61 ± 0.10	1.67 ± 0.26	0.852	
Cno	1.22 ± 0.10	—	—	
WT vs. *arm^{MZ}* and *cno^{MZ}* vs. *arm^{MZ}*				
	WT DV/AP	*arm^{MZ}* DV/AP	WT vs. *arm^{MZ}*	*arm^{MZ}* vs. *cno^{MZ}*
Nrt	0.94 ± 0.03	0.91 ± 0.03	0.561	0.040
aPKC	1.26 ± 0.14	1.87 ± 0.21	0.038	0.007
Baz	1.91 ± 0.22	2.17 ± 0.22	0.434	0.002
	WT AP/DV	*arm^{MZ}* AP/DV		
Myo	2.61 ± 0.33	1.88 ± 0.24	0.107	0.196
Cno	1.22 ± 0.10	1.17 ± 0.10	0.746	—
DMSO vs. cytoD				
	DMSO DV/AP	cytoD DV/AP	DMSO vs. *cytoD*	
Nrt	0.93 ± 0.01	0.83 ± 0.02	0.004[c]	
Arm	1.28 ± 0.04	1.47 ± 0.09	0.073	
DEcad	1.10 ± 0.05	1.48 ± 0.08	0.003	
aPKC	1.19 ± 0.08	1.61 ± 0.10	0.010	
Baz	1.60 ± 0.08	3.21 ± 0.15	<0.0001	

N = 5 embryos, from at least two different experiments.
[a]± SEM.
[b]p values of comparisons of degree of planar polarity between different genotypes or conditions, as determined by Student's *t* test.
[c]The planar polarization of Nrt in *arm^{MZ}* and after cytoD treatment may reflect partial failure of the restriction of Nrt to the basolateral domain (Harris and Peifer, 2004), perhaps in a planar-polarized way.

TABLE 1: Comparing degrees of planar polarization among different genotypes and conditions.

ability to accumulate in a planar-polarized manner, and Cno is not essential for myosin planar polarization.

Cno loss subtly enhances AJ planar polarity

Cno and its mammalian homologue afadin both localize to AJs, and Cno can bind to DE-cadherin in vitro (Sawyer *et al.*, 2009). One hypothesis is that Cno regulates localization of AJ proteins, perhaps specifically affecting AP cell borders, where myosin detaches in its absence. In *cno^{MZ}* mutants AJ proteins remain at AP borders where myosin has detached (Figure 4 and Supplemental Figure 4, B and C), but this did not rule out more subtle changes in their localization. We thus quantitated Arm and DEcad planar polarization. Previous studies revealed subtle Arm and DEcad planar polarization in WT (Blankenship *et al.*, 2006; Harris and Peifer, 2007). In our hands, Arm has a trend toward slight DV enrichment in WT (Figure 6, E and N, red vs. yellow arrowheads; Supplemental Table S1), whereas we did not detect DEcad planar polarization in WT (Figure 6, G and N; Supplemental Table S1), perhaps due to differences in fixation or measurement. In *cno^{MZ}*, in contrast, both Arm and DEcad were noticeably planar polarized, with clear DV border enrichment (Figure 6, F and H, red vs. yellow arrowheads; also see Figure 6N, Table 1, and Supplemental Table S1). We also examined absolute levels of AJ proteins by immunostaining WT and mutant embryos together. Nrt was unchanged, whereas overall levels of DEcad and Arm were reduced about twofold on both AP and DV borders (Supplemental Table S2). However, this reduction is unlikely to disrupt cell adhesion, as heterozygous mutants for either gene are WT during GBE; in fact, no defects were observed in DEcad zygotic null mutants until after GBE (Tepass *et al.*, 1996). Thus Cno helps restrain planar polarization of cadherin–catenin complexes; this could be direct, or indirect via effects on actin and myosin.

Planar polarity of apical polarity proteins Baz and aPKC is dramatically enhanced in *cno*^{MZ}

Like myosin, the apical polarity protein Baz is an important player in GBE (Zallen and Wieschaus, 2004). The contractile apical actomyosin network we observed during GBE is reminiscent of that in one-cell *Caenorhabditis elegans* embryos (Munro *et al*., 2004). In *C. elegans,* this network plays a role in cell polarization; on fertilization, the actomyosin network contracts anteriorward, and "anterior Par" proteins, including Par3 (fly Baz) and aPKC, move anteriorly (Munro *et al*., 2004), suggesting the possibility the two may be coupled. Therefore, we tested the hypothesis that loss of Cno and the dramatic changes in the apical actomyosin network would affect Baz and aPKC localization.

Baz initially colocalizes with DEcad in spot AJs (Harris and Peifer, 2005) and then becomes planar-polarized during GBE, with enrichment on DV borders with AJ proteins. It is striking that Baz planar polarity is *very* strongly enhanced in *cno*^{MZ}, increasing from approximately twofold to ninefold (Figure 6, I vs. J, red vs. yellow arrowheads; also see Figure 6N, Table 1, and Supplemental Table S1). We also measured absolute Baz levels at AP and DV borders in WT and *cno*^{MZ}, immunostaining them together and quantitating fluorescence. Although Baz is only slightly reduced on DV borders in *cno*^{MZ} relative to WT (13% less; Supplemental Table S2), it is substantially reduced on AP borders (60% less; Supplemental Table S2), suggesting that enhanced planar polarity is primarily due to Baz loss from AP borders (Figure 6J). We cannot exclude the possibility that the techniques we used (immunofluorescence and SEM) missed slight cell separation apically, which might contribute to apparent Baz reduction, but we think this less likely, as we measured multiple planes in the *z*-axis. Thus Cno function is required to retain Baz at AP borders, preventing its excess planar polarization.

Along DV cell borders, we observed another dramatic change in Baz localization in *cno*^{MZ} mutants. Although Baz remained enriched at DV borders in *cno*^{MZ}, it was largely restricted to central regions and did not extend to vertices where DV met AP borders (marked by Nrt; Figure 7, A–A″, arrows). In contrast with Baz, AJ proteins like Arm are not restricted to central DV borders and extend all the way to cell vertices (Figure 7B′, arrows). It is striking that Baz localization along DV borders did not extend past the myosin cables that were detached from AP border AJs (Figure 7, C and D, arrows). This raises the possibility that Baz localization may be influenced by, or influence, myosin localization.

To determine whether these changes in localization were particular for Baz or affected other apical polarity proteins, we examined aPKC. aPKC localizes apically to Baz and AJs during early gastrulation (Harris and Peifer, 2005), but its planar polarization during GBE had not been assessed. We found that aPKC is enriched with Baz on DV borders in WT (Figure 6K, red vs. yellow arrowheads; also see Figure 6N). It is striking that aPKC planar polarity is also strongly enhanced in *cno*^{MZ} (Figure 6L, red vs. yellow arrowheads; also see Figure 6N, Table 1, and Supplemental Table S1); like Baz, aPKC appeared reduced on AP borders. Furthermore, like Baz and unlike AJ proteins, aPKC was restricted to central DV borders in *cno*^{MZ} (Figure 7A‴, arrows). Thus Cno is required for correct planar polarization of both Baz and aPKC. These data raise the possibility that apical actomyosin may be coupled in some way to Baz and aPKC, as Cno loss affects their localization in parallel.

Mesoderm influences ectodermal cell shape change in the first 10 min of GBE (Butler *et al*., 2009). Although we had ruled out a role for Cno in this early cell shape change, to be certain that failure to fully invaginate mesoderm did not contribute to alterations in myosin and Baz localization in *cno*^{MZ}, we examined myosin and Baz in *fog* mutants, which do not complete mesoderm invagination. Fog acts via a completely different mechanism than Cno, acting as the ligand in a signaling pathway that triggers apical myosin accumulation and apical constriction of the mesoderm (Harris *et al*., 2009). In *fog* mutants we found that myosin cables do not detach from AP AJs, and Baz planar polarization is not dramatically altered (Supplemental Figure 6, C–E), confirming that the changes we see in *cno*^{MZ} (Supplemental Figure 6F) aren't solely due to defective mesoderm invagination. Together, these data suggest that Cno is required to properly maintain Baz and aPKC at AP borders and prevent their excessive planar polarization.

Globally reducing cell adhesion does not closely mimic Cno loss

Our data suggest that Cno helps to maintain integrity of the apical actomyosin network and couple it to AJs, disrupting this network impairs cell shape change and GBE, and Cno also helps to maintain normal Baz and aPKC localization and planar polarization. We next explored the mechanisms by which Cno regulates GBE, actomyosin, and planar polarity. We tested three hypotheses. First, Cno might be essential for cell adhesion, as suggested for mammalian afadin (Takai *et al*., 2008). Second, Cno might affect actomyosin. Third, Cno might cooperate with Baz in this process.

To test the hypothesis that reduced adhesion explains the effects of Cno loss, we examined embryos with globally reduced cell adhesion. We used embryos maternally/zygotically mutant for the strong allele *arm*^{043A01}, which have severely reduced Arm function (*arm*^{MZ}; null *arm* alleles disrupt oogenesis; Peifer *et al*., 1993). In *arm*^{MZ} mutants, epithelial integrity is lost during late GBE, as cells lose adhesion to neighbors (Figure 8, A vs. C). In contrast, *cno*^{MZ} mutants maintain epithelial integrity (Figure 8, A vs. B; Sawyer *et al*., 2009), suggesting that any role of Cno in adhesion is less critical than that of Arm. However, one can examine *arm*^{MZ} mutants during early to mid GBE, before the ectodermal epithelium disintegrates (Dawes-Hoang *et al*., 2005; Martin *et al*., 2010).

We explored whether globally reducing AJ function mimics the effects of Cno loss during early GBE, before *arm*^{MZ} mutants lose epithelial integrity. First we examined myosin cables at AP cell borders. In *arm*^{MZ}, myosin planar polarity is not altered (Figure 8L and Table 1), and initially myosin cables remain tightly associated with AJs on AP borders (Figure 8D, arrows), thus resembling WT (Figure 8E, arrows). This contrasts with widespread cable detachment at AP cell borders in *cno*^{MZ} (Figure 8F, arrows). Myosin localized normally to puncta at the center of some rosettes in *arm*^{MZ} (Figure 8G, arrow). However, as GBE progressed, although some groups of cells retained normal myosin localization (Figure 8H, yellow arrows), myosin was preferentially disrupted at AP boundaries (Figure 8H, blue arrows), as epithelia began to disintegrate (Figure 8C). Thus strongly reducing AJ function does not affect apical actomyosin anchoring as rapidly as does as Cno loss, but it ultimately disrupts myosin cables anchored at AJs.

We next examined localization of Cno, Baz, and aPKC in *arm*^{MZ} (Arm and DEcad levels are strongly reduced in *arm*^{MZ}, preventing examination; Dawes-Hoang *et al*., 2005; Sawyer *et al*., 2009). Cno planar polarity is not affected in *arm*^{MZ} (Figure 8L and Table 1). Of interest, Baz localization also was not substantially altered during early GBE in *arm*^{MZ}—Baz planar polarity remained unchanged (Figure 8L and Table 1), Baz was retained on AP borders (Figure 8, J′ vs. I′, yellow arrows), and on DV borders Baz extended to vertices (Figure 8, J′ vs. I′, arrowheads). This is in strong contrast with *cno*^{MZ}, where Baz was strongly reduced on AP borders (Figure 8K, arrows) and was restricted to central DV borders (Figure 8K,

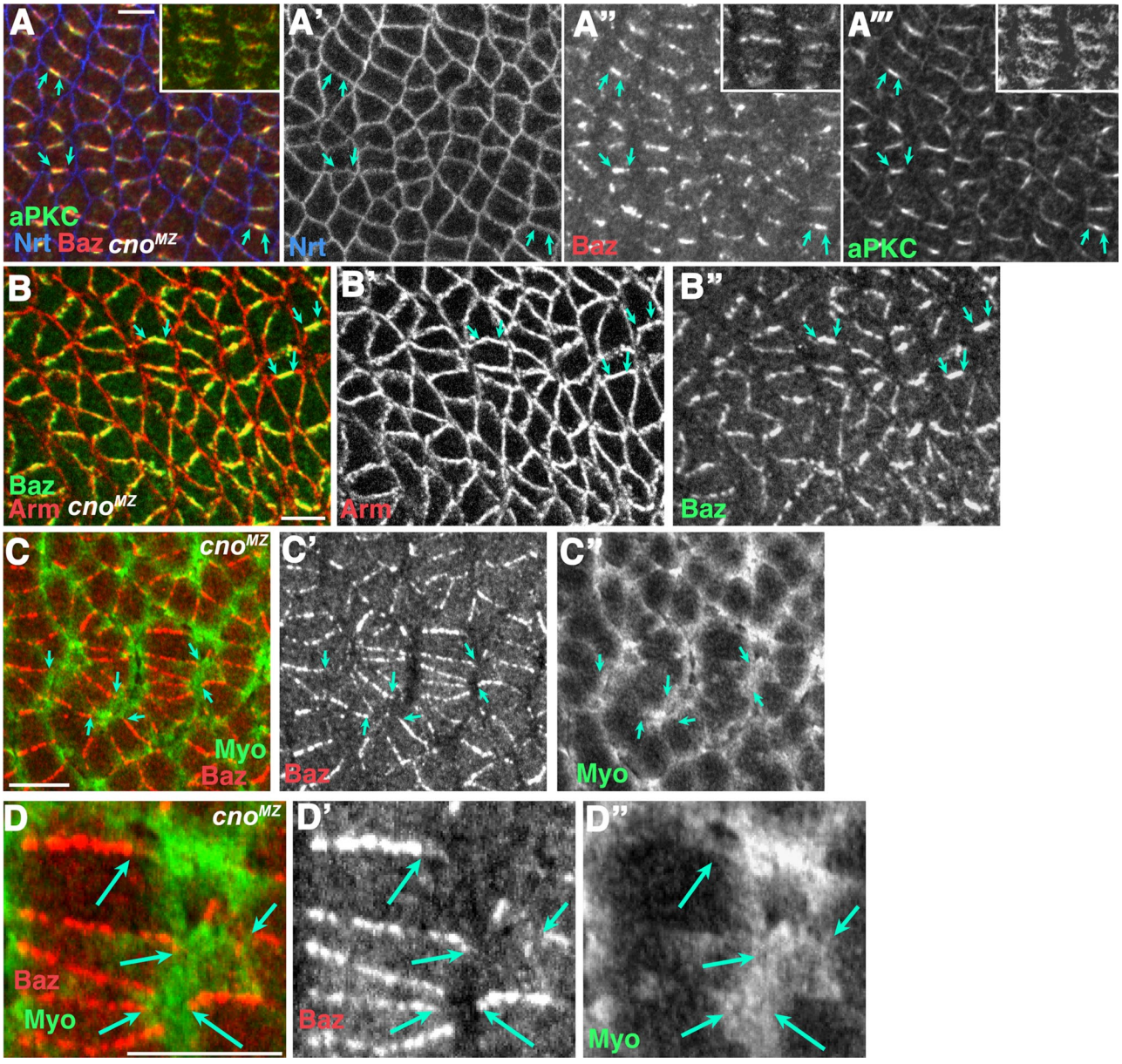

FIGURE 7: Changes in Baz and aPKC localization in cno^{MZ} mutants parallel actomyosin retraction. Stage 7 cno^{MZ} mutants, antigens indicated. (A) Baz and aPKC often localize only to central DV borders (arrows), not reaching vertices with AP borders. (B) Arm (B′, arrows) is not similarly restricted but extends all the way to vertices. (C, D) Baz along DV borders often only reaches edge of detached myosin cables (arrows) (D, close-up). Bars, 5 μm.

arrowheads). aPKC planar polarity was enhanced in arm^{MZ} (Figure 8L and Table 1), but this enhancement was substantially weaker than in cno^{MZ} (Figure 8L and Table 1). In contrast to cno^{MZ} (Figure 8K″), aPKC was not restricted to central DV borders in arm^{MZ} (Figure 8, J″ vs. I″). Thus globally reducing adhesion does not have the striking effects on Baz and aPKC localization that we saw in cno^{MZ}.

Globally reducing cell adhesion also does not mimic effects of Cno loss on cell shape. Unlike cno^{MZ}, in which cell elongation along the AP axis is impaired, in early GBE, arm^{MZ} cells elongated as much along the AP axis as WT (Supplemental Figure S2B), and arm^{MZ} cells have normal apical areas (Supplemental Figure S2D). Unlike both cno^{MZ} and WT, arm^{MZ} cells also elongated along the DV axis (Supplemental Figure S2B), perhaps because cells round up as adhesion fails. Consistent with this, arm^{MZ} cells also have larger apical areas than WT or cno^{MZ} before GBE (Supplemental Figure S2C), perhaps due to reduced apical tension (Martin *et al.*, 2010). Thus globally reducing adhesion alone does not phenocopy the changes in cell shape or protein localization observed in cno^{MZ} mutants. However, it remains possible that in cno^{MZ}, adhesion is reduced in a planar-polarized way along AP borders, and this asymmetric loss of adhesion accounts for phenotypes observed in cno^{MZ}.

Globally reducing F-actin partially mimics Cno loss

We next tested the hypothesis that Cno's primary role is to regulate apical actomyosin, by disrupting actin with the actin-depolymerizing drug cytochalasin D (cytoD) during early GBE. DEcad and Baz become planar polarized prematurely in cytoD-treated embryos (Harris and Peifer, 2005). In this study we examined the effects of actin depolymerization in more detail, quantitating planar polarization. cytoD strongly reduced cortical actin, as expected (Supplemental Figure S7, A and B). This, in turn, strongly reduced cortical myosin

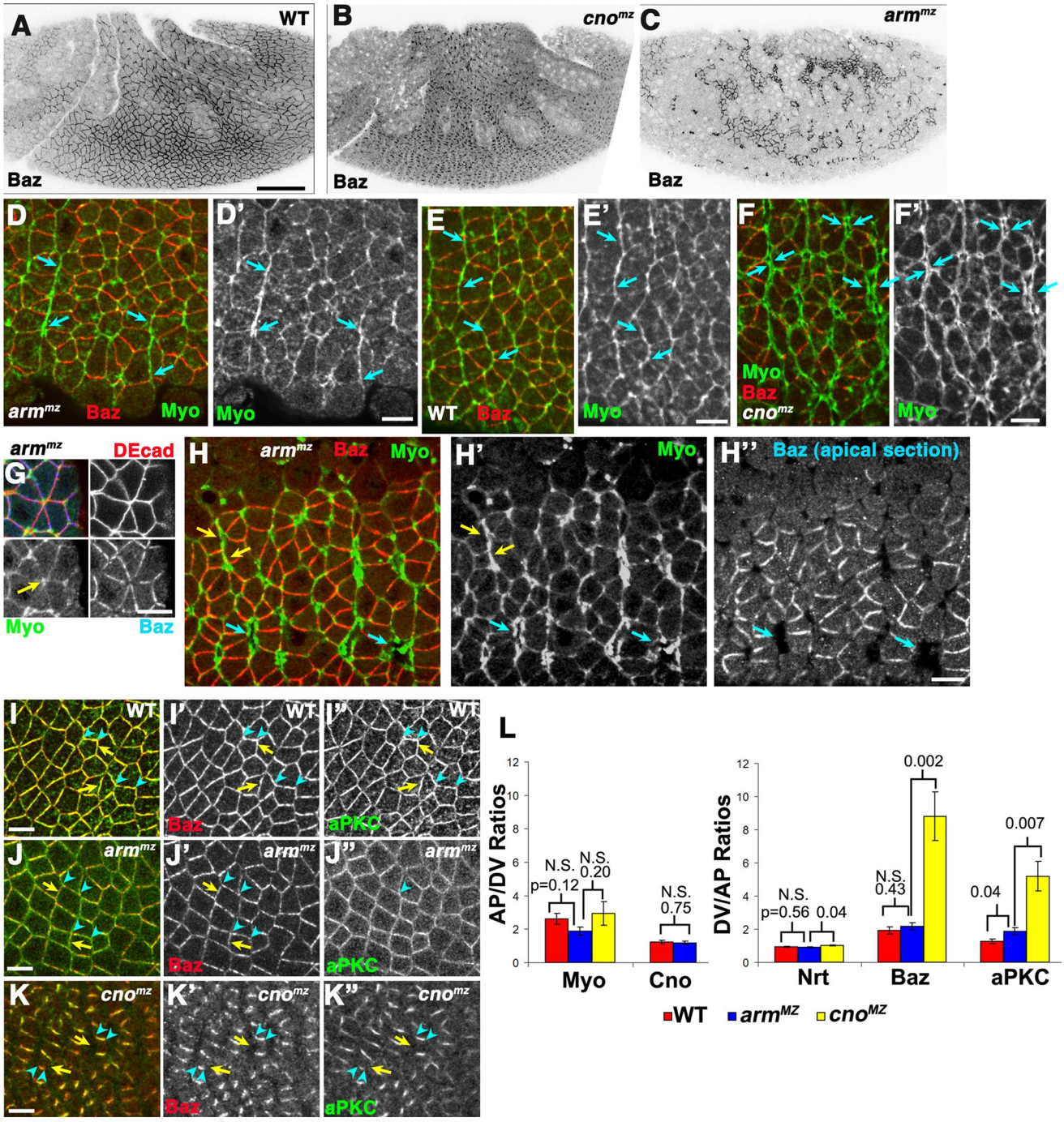

FIGURE 8: Globally reducing cell adhesion does not mimic Cno loss. (A–C) Stage 8. (D–K) Stage 7. (A–C) Arm reduction (C) but not Cno loss (B) leads to widespread disruption of cell adhesion and epithelial integrity during early stage 8. (D–F) In arm^{MZ} myosin initially remains in attached cortical cables (D, arrows), as in WT (E, arrows) but in contrast to cno^{MZ} (F, arrows). (G) In arm^{MZ}, some rosettes retain tight myosin localization to the vertex (arrow). (H) As GBE continues, arm^{MZ} cells begin to separate, and many myosin cables detach (blue arrows). However, some cables remain tightly cortical (yellow arrows). (I–K) Baz and aPKC are retained on AP borders in arm^{MZ} (J, yellow arrows) and extend all along DV borders (J, blue arrowheads), more resembling WT (I) than cno^{MZ}(K). (L) Planar polarity quantitation. Bars: A–C, 20 μm; D–L, 5 μm.

(Supplemental Figure S7, C vs. D, arrows), preventing assessment of its planar polarity. Like Cno loss (Figure 6N), however, cytoD treatment subtly enhanced DEcad and Arm planar polarity (Supplemental Figure S7, E′–H′, yellow vs. red arrowheads; Supplemental Figure S7K and Table S1; and unpublished data). It is striking that actin depolymerization also had effects similar to Cno loss on Baz and aPKC planar polarity, increasing both (Supplemental Figure S7, G″ vs. H″, I″ vs. J″; yellow vs. red arrowheads; Supplemental Figure S7K and Table S1). cytoD treatment made Baz localization less continuous on DV borders; however, the obvious retraction of Baz and aPKC from vertices seen in cno^{MZ} is not apparent.

Effects of actin depolymerization or Cno loss on cell shape change were also roughly similar. Both reduced AP cell elongation during early GBE (Supplemental Figure S2B). In fact actin depolymerization

had even more dramatic effects, with AP and DV borders remaining almost the same length. In addition, both actin depolymerization and Cno loss reduced apical area during early GBE relative to WT or dimethyl sulfoxide (DMSO)-treated controls (Supplemental Figure S2D). Taken together, these results suggest that disrupting the cytoskeleton more closely mimics Cno loss than does global reduction in cell adhesion. However, global cytoskeletal disruption did not precisely phenocopy Cno loss, perhaps because Cno preferentially regulates AJ:cytoskeleton connections along AP cell borders.

cno and *baz* exhibit strong, dose-sensitive genetic interactions

We then tested the hypothesis that Cno cooperates with Baz during GBE. One method of assessing whether two proteins work in a common cell biological process is to look for dose-sensitive genetic interactions, in which lowering levels of one protein enhances effects of reducing levels of another. Whereas maternal/zygotic *baz* mutants lose cell adhesion at gastrulation (Harris and Peifer, 2004), zygotic *baz* mutants, which retain maternal Baz, maintain epithelial integrity past GBE, and >90% have only modest defects in integrity of the epidermal epithelium later, as revealed by holes in the cuticle secreted by the epidermis (Shao *et al.*, 2010; Figure 9, A and B). This phenotype is enhanced by 50% reduction (maternal/zygotic heterozygosity) of known Baz-binding partners like DEcad, aPKC, and Crumbs (Shao *et al.*, 2010), demonstrating that phenotypic enhancement can indicate cooperation with Baz. *cno* is recessive, and thus flies with 50% reduced Cno levels (maternal/zygotic heterozygotes) are adult viable with no noticeable defects.

We thus tested the hypothesis that Cno cooperates with Baz during GBE by assessing whether reducing Cno levels by 50% (using *cno* heterozygous mothers) modifies effects of reducing Baz. To do so, we crossed females heterozygous for both genes to WT males; all progeny thus had reduced maternal levels of both proteins, and because *baz* is on the X chromosome, 25% were zygotically *baz* mutant, whereas none were *cno* zygotic mutants. Reducing Cno levels strongly enhanced *baz*'s phenotype. The fraction of embryos with severe cuticular integrity defects (Figure 9, C–E) increased from 5% in *baz* mutants alone to 59% in *baz* mutants with reduced Cno levels (Figure 9F). Thus *cno* and *baz* exhibit strong dose-sensitive genetic interactions.

In contrast, reducing Cno levels didn't enhance the phenotype of zygotic myosin heavy chain mutants (= *zipper*); there was no change in severity of *zipper's* cuticle phenotype (32% mild/68% severe defects vs. 35% mild/65% severe defects). However, absence of a dose-sensitive interaction is not evidence for or against a functional relationship, as it depends on relative levels of maternal and zygotic gene product.

To explore the cell biological mechanisms by which this *baz cno* genetic interaction affects development, we compared morphogenesis in *baz* zygotic mutants versus *baz* mutants with reduced Cno levels, generated using the cross outlined previously. In *baz* mutants, epidermal AJs remain largely intact through the extended germband stage (Shao *et al.*, 2010; Figure 9, G vs. L). Reducing Cno levels promoted earlier disruption of AJs; 21% of extended germband embryos mutant for *baz* and with reduced Cno had moderate to strong AJ disruption (n = 66; Figure 9, H and I, arrowheads) versus 8% of *baz* mutants (n = 63). Most strikingly, 47% of *baz* mutants with reduced Cno levels had a partially open ventral furrow (n = 49; Figure 9, I–K), suggesting a possible failure of apical constriction. This phenotype was never observed in *baz* mutants (n = 27) but is characteristic of cno^{MZ} mutants (Sawyer *et al.*, 2009). Thus *baz* and *cno* exhibit strong, dose-sensitive genetic interactions from gastrulation onward, consistent with the two proteins cooperating in the same process.

DISCUSSION

Coordinating adhesion and the cytoskeleton is essential for morphogenesis. Recent work on apical constriction provides a model of how cell shape change is coupled to actomyosin contractility. Our data suggest that coupling AJs to a contractile apical actomyosin cytoskeleton plays an important role in a very different cell movement: convergent extension during *Drosophila* GBE. We identified a novel cell shape change, AP cell elongation, which contributes to WT GBE. Furthermore, we found that Cno is required for maintaining attachment of the apical actomyosin network AJs in a planar-polarized way. Disrupting this connection results in failure of GBE and prevents coordination of apical myosin contractility and cell shape change. Our data are consistent with a model in which Cno tightly couples apical actomyosin to AP AJs and coordinates apical polarity proteins with the network, helping to integrate individual cell shape changes across the tissue.

A dynamic apical actomyosin network as a general feature of cell intercalation

Previous studies illustrated how an apical contractile actomyosin network powers apical constriction (reviewed in Sawyer *et al.*, 2010). In contrast, convergent extension during *Drosophila* GBE was thought to involve planar-polarized enhancement of contractile actomyosin cables, driving cell intercalation and body elongation (Zallen and Blankenship, 2008). We were surprised to find that, in addition to junctional cables, germband cells also have an apical actomyosin network that undergoes cyclical constriction and relaxation. This coincides with and may help to drive cell shape change. The asymmetric cue of planar-polarized myosin is likely to impose asymmetry. Together, asymmetric cortical myosin and cyclical contractions may help to extend cells in one dimension instead of shrinking them in all dimensions, thus contributing to tissue elongation. While this manuscript was being revised, Lecuit's and Zallen's labs independently discovered and described the apical network—the Lecuit lab data further suggest that myosin condensations preferentially move toward AP borders, helping to drive cell rearrangement (Rauzi *et al.*, 2010; Fernandez-Gonzalez and Zallen, 2011). Both our data on Cno and the Lecuit lab's data on α-catenin further suggest that different proteins linking this apical network to AJs are critical for the fidelity and coupling of apical myosin contraction to cell shape change.

We also identified a novel cell shape change that may help to drive AP body axis extension—AP cell elongation. Cno and presumably linkage of the apical actomyosin network to AJs are important for this cell shape change. One speculative possibility is that an asymmetric ratchet acts in germband cells, selectively preventing elongation along the DV body axis while allowing cell elongation along the AP body axis. It is also possible that outside forces, such as shape changes of the first cells to divide, help reshape ectodermal cells, but we think that this is less likely, as we examined cell shapes during early GBE before germband mitotic domains divide. Ratchets have also been proposed during mesoderm invagination (Martin *et al.*, 2009) and during dorsal closure, where amnioserosal cells apically constrict (Solon *et al.*, 2009). Before dorsal closure onset, amnioserosal cells have periodic apical actomyosin contractions, but cells only retain changes in shape after a junctional actomyosin purse string appears. Disrupting the purse string disrupts dorsal closure, suggesting that a junctional actomyosin cable can act as a ratchet.

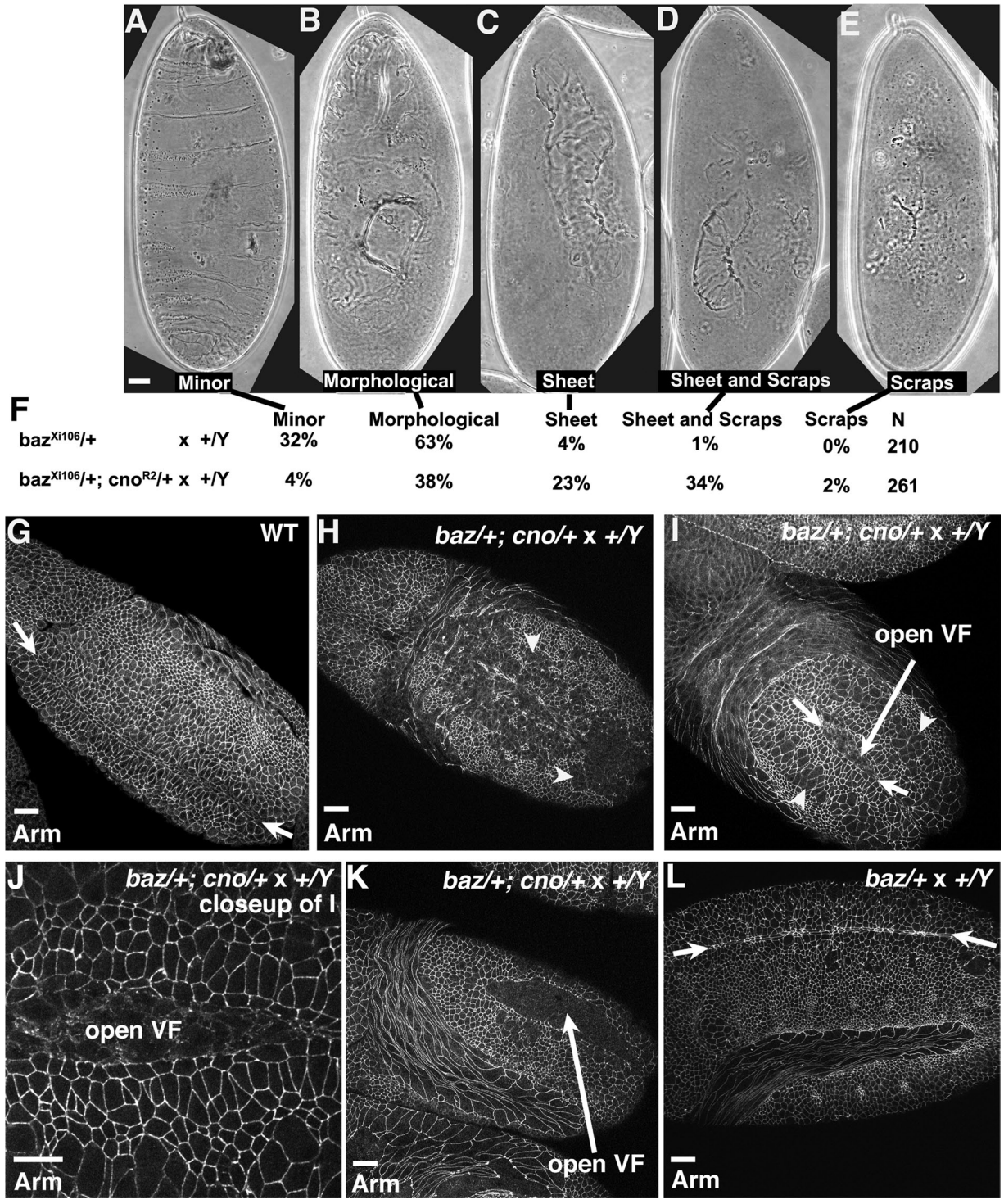

FIGURE 9: Reducing Cno levels enhances the phenotype of zygotic *baz* mutants. (A–E) Cuticle preparations illustrating different phenotypes seen in progeny. (F) Reducing Cno enhances the *baz* phenotype. In both cases, we analyzed *baz* zygotic mutant progeny. In the top cross, embryos had wild-type levels of maternal and zygotic Cno. In the bottom cross, levels of maternal Cno were reduced by 50% (note that no embryos in this cross are homozygous mutant for *cno*). (G–L) Stage 9–11 embryos of the indicated genotypes. Reducing Cno leads to earlier defects in epithelial integrity in *baz* mutants (arrowheads indicate epithelial disruption) and also leads to failure of mesoderm invagination in many embryos. Arrows indicate closed (G, L) or open (I, K) ventral furrows. Bars, 20 μm.

Studies in *Xenopus* suggest that the role of a dynamic, planar-polarized apical actomyosin network in convergent extension is conserved (Skoglund *et al.*, 2008; Kim and Davidson, 2011). Myosin organizes actin into dynamic foci that move within intercalating cells along their mediolateral axis. In myosin's absence, actin foci are lost and convergent extension is disrupted. Thus

dynamic actomyosin foci may play a conserved role in convergent extension.

It will be interesting to identify regulators shaping contractile activity in different tissues. Jak/Stat signaling restricts apical constriction to the mesoderm (Bertet *et al.*, 2009); in its absence apical myosin accumulates in the ectoderm, and those cells inappropriately apically constrict. Thus, although both mesoderm and ectoderm share an apical contractile network, its regulation is tuned differently. Furthermore, different actin regulators regulate apical and junctional myosin, with Wasp regulating the apical pool.

Cno: one of several important players linking AJs to actin during gastrulation

Linking AJs to actin is key in diverse processes from adhesion itself to morphogenetic movements as different as apical constriction and collective cell migration (Gates and Peifer, 2005). Cno regulates linkage during mesoderm apical constriction, but isn't required for cell adhesion (Sawyer *et al.*, 2009). Other AJ-actin linkers act in other contexts (e.g., Abe and Takeichi, 2008; Cavey *et al.*, 2008), suggesting that cells use distinct linkers in circumstances with different force regimes. Our data suggest that during GBE, Cno regulates AJ:actomyosin network connections, acting specifically along AP borders.

Core AJ proteins are more reduced on AP borders in cno^{MZ} mutants than in WT. In WT, slightly reducing AJ proteins on AP borders may facilitate shrinkage of these borders during GBE. It is tempting to speculate that Cno enhancement along AP borders provides extra support when DEcad/Arm is reduced, strengthening AJ:actomyosin linkages along AP borders yet still allowing cell shape change. In this model, when Cno is absent, AJ:actomyosin linkage is weakened at AP borders, leading to inefficient cell shape change, impairing GBE, and accentuating reduction of AJ proteins.

Our data further suggest that Cno is not the only AJ:actomyosin linker during GBE. Although the actomyosin network detaches from AJs in cno^{MZ}, it does not collapse into a ball; instead, cables remain 0.2–0.5 μm distant from AJs. A second connection is also supported by the appearance of apical strands of DEcad stretching from the cortex to detached myosin in cno^{MZ}. It will be interesting to determine what proteins compose these other AJ:actomyosin links. α-Catenin regulates actin:AJ linkage just prior to this stage (Cavey *et al.*, 2008) and also plays a role in GBE (Rauzi *et al.*, 2010), although how α-catenin mediates linkage remains mysterious.

Coordinating actomyosin and apical polarity proteins: a conserved contractility modulator?

Both myosin and Baz/Par3 are important GBE regulators (Bertet *et al.*, 2004; Zallen and Wieschaus, 2004). One of the most surprising consequences of Cno loss was dramatic change in Baz and aPKC localization. Their strong reduction along AP borders and restricted localization along DV borders correlates well with altered localization of apical actomyosin, which detached from AP AJs and retracted along DV borders from vertices. These data suggest that coordination of the actomyosin network and Baz/aPKC facilitates efficient cell shape change. Consistent with this, an interesting recent paper demonstrated that Baz is required for reciprocal planar-polarized distribution of myosin and AJs. Baz localization, in turn, is restricted by the cytoskeletal regulator Rho-kinase (Rok), leaving Baz enriched at DV borders (Simoes Sde *et al.*, 2010). This suggests a complex network of interactions.

In *C. elegans* a contractile actomyosin cytoskeleton positions apical-polarity proteins (PAR3/PAR6/aPKC) anteriorly in one-cell embryos, and this complex then alters the actomyosin network, promoting asymmetric cortical flow to maintain anterior and posterior domains (Munro *et al.*, 2004). It is tempting to speculate that the germband contractile actomyosin network plays a similar role. In this model, planar polarization of the network would create a symmetry break (Bertet *et al.*, 2004; Blankenship *et al.*, 2006; Simoes Sde *et al.*, 2010), helping to trigger Baz/aPKC planar polarization. They, in turn, may feed back to modulate actomyosin contractility, driving GBE. Strengthening AJ:actomyosin linkages via Cno could help to ensure efficient cell shape changes that are integrated across the tissue.

Several mechanistic hypotheses are consistent with our data, which are not mutually exclusive. First, Cno may directly affect Baz/aPKC localization during assembly or maintenance, working in parallel or in series with Rok (Simoes Sde *et al.*, 2010), with actomyosin positioning and contractility then modulated by Baz/aPKC. Consistent with this, previous work revealed that Baz remains apical in the absence of AJs; residual epithelial cells retain polarized actin but have hyperconstricted apical ends (Harris and Peifer, 2004). Furthermore, PAR proteins regulate actomyosin contractility during DC (David *et al.*, 2010). Second, Cno could alter the actomyosin network, which in turn may affect proper Baz/aPKC localization. Baz apical positioning requires the actin cytoskeleton (Harris and Peifer, 2005). We found actin disruption and Cno loss alter Baz localization similarly, consistent with this hypothesis. Finally, Baz/aPKC may mediate Cno apical positioning, as Baz does for AJs (Harris and Peifer, 2004). Of course, more complex interplay with feedback between actomyosin and Baz/aPKC seems likely, creating a network of interactions rather than a linear pathway. Teasing out the complex coordination of AJs, apical polarity protein, and the actomyosin network during morphogenesis is an exciting challenge.

MATERIALS AND METHODS

Flies

Mutations/fly stocks are described at FlyBase (http://flybase.org/) and in Supplementary Table S4. WT is *yellow white*. Experiments were done at 25°C unless noted otherwise. The *cno* germline clones were made by heat shocking 48- to 72-h $hsFLP^{1}$;FRT82Bcno^{R2}/FRT82B$ovo^{D1–18}$ larvae for 3 h at 37°C. The arm^{043A01} germline clones were generated similarly.

Microscopy

Antibodies are in listed in Supplementary Table S4. Embryo fixation, preparation, and drug treatments were as in Sawyer *et al.* (2009). For SEM, embryos were dechlorionated with 50% bleach, fixed for 5 min in 37% formaldehyde, hand devitillinized, and post-fixed in 2.5% gluteraldehyde:0.1 M cacodylate; specimens were prepared by the University of North Carolina's Microscopy Services Laboratory and imaged on a Zeiss (Thornwood, NY) Supra 25 field emissions microscope. Fixed samples were imaged with a Zeiss LSM 510, a Zeiss 40× Plan-NeoFluar numerical aperture (NA) 1.3 oil immersion objective, and LSM software. Live imaging was performed with a PerkinElmer (Waltham, MA) UltraView spinning disk confocal ORCA-ER camera, Nikon (Melville, NY) 60× Plan Apo NA 1.4 or 100× Plan ApoVC NA 1.4 objectives, and MetaMorph software (Molecular Devices, Sunnyvale, CA). Four-dimensional differential interference contrast (DIC) imaging used a Diagnostic Instruments (Sterling Heights, MI) SPOT 2 camera and Nikon Eclipse E800 microscope with a 20× Nikon Plan Fluor DIC infinity-corrected NA 0.5 objective. The 11-μm optical sections were acquired every 2 min for 5 h and analyzed with MetaMorph. In Adobe (San Jose, CA) Photoshop CS2 we adjusted input levels so the main range of

signals spanned the entire output grayscale and adjusted brightness and contrast.

Quantification of planar polarity and cell shape change

Stacks from stage 7 to early stage 8 embryos were acquired with a Zeiss 40× Plan-NeoFluar NA 1.3 oil immersion objective, zoom 2. Mean fluorescence intensities of all borders (zoom 300%) were measured with ImageJ's (National Institutes of Health, Bethesda, MD) line tool (line width, 3). To ensure that the entire border was measured, stacks of four planes 0.5 µm apart were used, and measurements were averaged to obtain border value, with background (measured similarly, but in the cytoplasm) subtracted to obtain the final value. Borders were sorted by angles (relative to embryo DV axis). AP borders, 0°–29°; DV, 60°–90°. Ratios from embryos from two or more experiments were averaged. Cell border lengths and areas were similarly measured.

Automated analysis of apical myosin accumulation and cell area

To obtain the data analyzed in Figure 3, time-lapse images of DEcad-GFP were first processed using ImageJ software in the following steps: 1) Image background was first subtracted by the rolling ball algorithm function with a radius of 50. 2) Remaining background noise and irrelevant dim particles were further subtracted by direct subtraction. 3) The resulting images were filtered by a Gaussian blur filter with radius of three to four pixels and segmented by watershed segmentation plug-in. 4) Segmented images were corrected manually based on the original images. The segmented images were analyzed by MATLAB (MathWorks, Natick, MA) to track each cell, measure cell area, and calculate average Spaghetti Squash (Sqh)–mCherry intensity within the area. To analyze changes over time, time-series data of cell area and average Sqh-mCherry intensity were first smoothed by a Gaussian filter with a width of five data points in MATLAB software, and intervals between neighboring peaks were calculated. For area reduction, because we were interested in cell constriction, the inverse of the changes was used. The r was calculated with time offsets from −200 to +200 s as previously described (He *et al.*, 2010). The heat map was constructed by correlations of different individual cells with coefficients coded in rainbow color. Two-sided *t* test with unequal variance was conducted in Microsoft Excel (Redmond, WA). All error bars are SD of the mean (SDM).

ACKNOWLEDGMENTS

We thank the Bloomington stock center, Developmental Studies Hybridoma Bank, J. Zallen, and E. Wieschaus for reagents; J. Zallen, T. Harris, E. Munro, and A. Martin for helpful discussions; V. Madden of the University of North Carolina for assistance with SEM; J. M. Sawyer for assistance with DIC; and M. Duncan, B. Duronio, and S. Rogers for critical reading of the manuscript. This work was supported by National Institutes of Health Grant R01GM47957 to M.P. J.K.S. was supported in part by an American Heart Association predoctoral fellowship.

REFERENCES

Abe K, Takeichi M (2008). EPLIN mediates linkage of the cadherin catenin complex to F-actin and stabilizes the circumferential actin belt. Proc Natl Acad Sci USA 105, 13–19.

Bertet C, Rauzi M, Lecuit T (2009). Repression of Wasp by JAK/STAT signalling inhibits medial actomyosin network assembly and apical cell constriction in intercalating epithelial cells. Development 136, 4199–4212.

Bertet C, Sulak L, Lecuit T (2004). Myosin-dependent junction remodelling controls planar cell intercalation and axis elongation. Nature 429, 667–671.

Blankenship JT, Backovic ST, Sanny JS, Weitz O, Zallen JA (2006). Multicellular rosette formation links planar cell polarity to tissue morphogenesis. Dev Cell 11, 459–470.

Butler LC, Blanchard GB, Kabla AJ, Lawrence NJ, Welchman DP, Mahadevan L, Adams RJ, Sanson B (2009). Cell shape changes indicate a role for extrinsic tensile forces in *Drosophila* germ-band extension. Nat Cell Biol 11, 859–864.

Cavey M, Rauzi M, Lenne PF, Lecuit T (2008). A two-tiered mechanism for stabilization and immobilization of E-cadherin. Nature 453, 751–756.

da Silva SM, Vincent JP (2007). Oriented cell divisions in the extending germband of *Drosophila*. Development 134, 3049–3054.

David DJ, Tishkina A, Harris TJ (2010). The PAR complex regulates pulsed actomyosin contractions during amnioserosa apical constriction in *Drosophila*. Development 137, 1645–1655.

Dawes-Hoang RE, Parmar KM, Christiansen AE, Phelps CB, Brand AH, Wieschaus EF (2005). Folded gastrulation, cell shape change and the control of myosin localization. Development 132, 4165–4178.

Drees F, Pokutta S, Yamada S, Nelson WJ, Weis WI (2005). α-Catenin is a molecular switch that binds E-cadherin/β-catenin and regulates actin-filament assembly. Cell 123, 903–915.

Fernandez-Gonzalez R, Simoes Sde M, Roper JC, Eaton S, Zallen JA (2009). Myosin II dynamics are regulated by tension in intercalating cells. Dev Cell 17, 736–743.

Fernandez-Gonzalez R, Zallen JA (2011). Oscillatory behaviors and hierarchical assembly of contractile structures in intercalating cells. Phys Biol (*in press*).

Gates J, Peifer M (2005). Can 1000 reviews be wrong? Actin, alpha-catenin, and adherens junctions. Cell 123, 769–772.

Harris TJ, Peifer M (2004). Adherens junction-dependent and -independent steps in the establishment of epithelial cell polarity in *Drosophila*. J Cell Biol 167, 135–147.

Harris TJ, Peifer M (2005). The positioning and segregation of apical cues during epithelial polarity establishment in *Drosophila*. J Cell Biol 170, 813–823.

Harris TJ, Peifer M (2007). aPKC controls microtubule organization to balance adherens junction symmetry and planar polarity during development. Dev Cell 12, 727–738.

Harris TJ, Sawyer JK, Peifer M (2009). How the cytoskeleton helps build the embryonic body plan: models of morphogenesis from *Drosophila*. Curr Top Dev Biol 89, 55–85.

He L, Wang X, Tang HL, Montell DJ (2010). Tissue elongation requires oscillating contractions of a basal actomyosin network. Nat Cell Biol 12, 1133–1142.

Irvine KD, Wieschaus E (1994). Cell intercalation during *Drosophila* germband extension and its regulation by pair-rule segmentation genes. Development 120, 827–841.

Kim HY, Davidson LA (2011). Punctuated actin contractions during convergent extension and their permissive regulation by the non-canonical Wnt-signaling pathway. J Cell Sci 124, 635–646.

Martin AC, Gelbart M, Fernandez-Gonzalez R, Kaschube M, Wieschaus EF (2010). Integration of contractile forces during tissue invagination. J Cell Biol 188, 735–749.

Martin AC, Kaschube M, Wieschaus EF (2009). Pulsed contractions of an actin-myosin network drive apical constriction. Nature 457, 495–499.

Munro E, Nance J, Priess JR (2004). Cortical flows powered by asymmetrical contraction transport PAR proteins to establish and maintain anterior-posterior polarity in the early *C. elegans* embryo. Dev Cell 7, 413–424.

Peifer M, Orsulic S, Sweeton D, Wieschaus E (1993). A role for the *Drosophila* segment polarity gene *armadillo* in cell adhesion and cytoskeletal integrity during oogenesis. Development 118, 1191–1207.

Rauzi M, Lenne PF, Lecuit T (2010). Planar polarized actomyosin contractile flows control epithelial junction remodelling. Nature 468, 1110–1114.

Rauzi M, Verant P, Lecuit T, Lenne PF (2008). Nature and anisotropy of cortical forces orienting *Drosophila* tissue morphogenesis. Nat Cell Biol 10, 1401–1410.

Sawyer JK, Harris NJ, Slep KC, Gaul U, Peifer M (2009). The *Drosophila* afadin homologue Canoe regulates linkage of the actin cytoskeleton to adherens junctions during apical constriction. J Cell Biol 186, 57–73.

Sawyer JM, Harrell JR, Shemer G, Sullivan-Brown J, Roh-Johnson M, Goldstein B (2010). Apical constriction: a cell shape change that can drive morphogenesis. Dev Biol 341, 5–19.

Shao W, Wu J, Chen J, Lee DM, Tishkina A, Harris TJ (2010). A modifier screen for Bazooka/PAR-3 interacting genes in the *Drosophila* embryo epithelium. PLoS One 5, e9938.

Simoes Sde M, Blankenship JT, Weitz O, Farrell DL, Tamada M, Fernandez-Gonzalez R, Zallen JA (2010). Rho-kinase directs Bazooka/Par-3 planar polarity during *Drosophila* axis elongation. Dev Cell 19, 377–388.

Skoglund P, Rolo A, Chen X, Gumbiner BM, Keller R (2008). Convergence and extension at gastrulation require a myosin IIB-dependent cortical actin network. Development 135, 2435–2444.

Solon J, Kaya-Copur A, Colombelli J, Brunner D (2009). Pulsed forces timed by a ratchet-like mechanism drive directed tissue movement during dorsal closure. Cell 137, 1331–1342.

Takai Y, Ikeda W, Ogita H, Rikitake Y (2008). The immunoglobulin-like cell adhesion molecule nectin and its associated protein afadin. Annu Rev Cell Dev Biol 24, 309–342.

Tepass U, Gruszynski-DeFeo E, Haag TA, Omatyar L, Török T, Hartenstein V (1996). *shotgun* encodes *Drosophila* E-cadherin and is preferentially required during cell rearrangement in the neurectoderm and other morphogenetically active epithelia. Genes Dev 10, 672–685.

Yamada S, Pokutta S, Drees F, Weis WI, Nelson WJ (2005). Deconstructing the cadherin–catenin–actin complex. Cell 123, 889–901.

Yin C, Ciruna B, Solnica-Krezel L (2009). Convergence and extension movements during vertebrate gastrulation. Curr Top Dev Biol 89, 163–192.

Zallen JA, Blankenship JT (2008). Multicellular dynamics during epithelial elongation. Semin Cell Dev Biol 19, 263–270.

Zallen JA, Wieschaus E (2004). Patterned gene expression directs bipolar planar polarity in *Drosophila*. Dev Cell 6, 343–355.

Zallen JA, Zallen R (2004). Cell-pattern disordering during convergent extension in *Drosophila*. J Phys Condens Matter 16, S5073–S5080.